AWARD NUMBER: W81XWH-13-1-0203

TITLE: Targeting Palmitoyl Acyltransferases in Mutant NRAS-Driven Melanoma

PRINCIPAL INVESTIGATOR: Xu Wu, Ph.D.

CONTRACTING ORGANIZATION: Massachusetts General Hospital
Boston, MA 02114

REPORT DATE: October 2015

TYPE OF REPORT: Final

PREPARED FOR: U.S. Army Medical Research and Materiel Command
Fort Detrick, Maryland 21702-5012

REPORT DOCUMENTATION PAGE

Form Approved
OMB No. 0704-0188

1. REPORT DATE	2. REPORT TYPE	3. DATES COVERED
October 2015	Final	1Aug2013 - 31Jul2015

4. TITLE AND SUBTITLE
Targeting Palmitoyl Acyltransferases in Mutant NRAS-Driven Melanoma

5a. CONTRACT NUMBER

5b. GRANT NUMBER
W81XWH-13-1-0203

5c. PROGRAM ELEMENT NUMBER

6. AUTHOR(S)

Xu Wu, Ph.D

E-Mail: xwu@cbrc2.mgh.harvard.edu

5d. PROJECT NUMBER

5e. TASK NUMBER

5f. WORK UNIT NUMBER

7. PERFORMING ORGANIZATION NAME(S) AND ADDRESS(ES)

Massachusetts General Hospital
Boston, MA 02114

8. PERFORMING ORGANIZATION REPORT NUMBER

9. SPONSORING / MONITORING AGENCY NAME(S) AND ADDRESS(ES)

U.S. Army Medical Research and Materiel Command
Fort Detrick, Maryland 21702-5012

10. SPONSOR/MONITOR'S ACRONYM(S)

11. SPONSOR/MONITOR'S REPORT NUMBER(S)

12. DISTRIBUTION / AVAILABILITY STATEMENT

Approved for Public Release; Distribution Unlimited

13. SUPPLEMENTARY NOTES

14. ABSTRACT

Mutations in N-RAS are linked to ~20% of melanoma with no effective treatment. Targeting palmitoyl acyltansferases (PATs) involved in N-RAS regulation could be a novel strategy to treat N-RAS mutant melanoma. The objective of the project is to identify PATs responsible for NRAS activation in melanoma cells using chemical biology and functional genomic approaches. In the first year of the study, we have developed more potent chemical probes to profile PATs in cells, and have carried out PATs profiling in melanoma cells using chemical probes and mRNA profiling. We have identified candidate PATs highly expressed in NRAS melanoma cells. We have developed shRNA reagents to further study their functions.

15. SUBJECT TERMS
NRAS, Melanoma, Palmitoylation

16. SECURITY CLASSIFICATION OF:			17. LIMITATION OF ABSTRACT	18. NUMBER OF PAGES	19a. NAME OF RESPONSIBLE PERSON
a. REPORT	b. ABSTRACT	c. THIS PAGE			USAMRMC
U	U	U	UU	31	19b. TELEPHONE NUMBER *(include area code)*

Table of Contents

Page

1. **Introduction……...4**
2. **Keywords……...4**
3. **Accomplishments……..……....4**
4. **Impact……...…….....11**
5. **Changes/Problems...…..…….....11**
6. **Products…….……..…..…….11**
7. **Participants & Other Collaborating Organizations……12**
8. **Special Reporting Requirements……14**
9. **Appendices……14**

1. INTRODUCTION

Mutations in N-RAS are linked to ~20% of melanoma with no effective treatment, representing a large unmet medical need. Palmitoylation (post-translational modification by adding a 16-carbon palmitate) is required for N-RAS proper membrane localization and its oncogenic activities. Recently, 23 of DHHC (Asp-His-His-Cys)-family proteins were discovered as protein palmitoyl acyltransferases (PATs). Targeting DHHC-PATs involved in N-RAS regulation could be a novel strategy to treat N-RAS mutant melanoma. We have developed chemical probes that covalently label the active sites of DHHC-PATs, allowing us to investigate the enzymatic activities of PATs that are responsible for N-RAS palmitoylation using Activity-Based Protein Profiling (ABPP) approaches. The first objective is to identify DHHC-PATs regulating palmitoylation of oncogenic N-RAS in melanoma cells using ABPP methods and compare with the mRNA expression profile to identify candidate PATs highly active in NRAS mutant melanoma cells. The second objective is to evaluate the effects of shRNAs targeting DHHC-PATs on N-RAS activity, melanoma cell proliferation and apoptosis. Finally, we aim to design and synthesize analogues of cerulenin, a natural product inhibitor of PATs to identify small molecule inhibitors of N-RAS palmitoylation.

2. KEYWORDD

NRAS, melanoma, palmitoylation, DHHC domain containing palmitoyl acyltransferases, Activity based protein profiling (ABPP), proteomics

3. ACCOMPLISHMENTS

What were the major goals of the project?

The major goal of the project is to use chemical biology and functional genomics approaches to study palmitoyl acyltransferases involved in NRAS activation in melanoma cells. As we stated in the SOW of the grant, there are three major tasks of this project. Task1: To identify DHHC-PATs regulating palmitoylation of oncogenic N-RAS in melanoma cells (Month 1-12). Task2. To evaluate the effects of shRNAs targeting DHHC-PATs on NRAS activity, melanoma cell proliferation and apoptosis (Month 13-24). Task3. To design and synthesize analogues of cerulenin, a natural product inhibitor of palmitoyl acyltransferases to identify small molecule inhibitors of N-RAS palmitoylation. (in parallel with Task1 and 2, Month 0-24).

In the entire funding period, we have accomplished work proposed in Task 1, 2 and 3.

Below are the details of our activities regarding to the SOW.

What was accomplished under these goals?

Task 1a. Test the activity based probe (16C-BYA) for labeling efficiency in multiple N-RAS mutant melanoma cell lines (SK-Mel30, SK-Mel2, MEL-JUSO, BL, etc.) and control cell lines (BRAF mutant melanoma, A375, U62, MalMe, M14, SK-Mel5 and primary human melanocytes) in 6-well format, optimize the concentration and labeling time (month 1-6).

Accomplishments: We have tested the labeling of the probe 16C-BYA (alkyne-2-BP) in NRAS melanoma cells (SK-Mel30, SK-Mel2 and 501Mel), and compared the pattern of labeling with the control cell line A375, which carries BRAF mutation. The concentration and time of labeling has been optimized to 50uM of probe for 8 hours labeling. We have carried out Click chemistry using Biotin-Azide or Rhodamine-Azide, and have compared the labeling efficiency and pattern of the cell lines that we have studied. We found that the probe specifically labeled several bands in NRAS mutant cell lines, which might represent potential candidate palmitoyl acyltransferases regulating NRAS activities.

Task 1b. Proteomic and mass spectrometry analysis of labeled proteins (month 6-12).

Accomplishments: We have carried out large-scale labeling experiments under the oiptimized condition (100uM probe for 8hours labeling) using 5 dishes of 10cm dishes for SK-Mel2 and SK-Mel30 cells, which gave us sufficient proteins for follow-up proteomics studies. We carried out Click chemistry using Biotin-azide, and used Streptavidin bead to enrich the labeled protein. We carried out on-bead digestion using trysin and the peptides were submitted to Harvard Medical School Taplin Mass Spectrometry center for protein identification. We successfully finished the proteomics studies, and our studies suggested that 3 DHHC proteins were among the palmitoyl acyltransferases with high activities in the NRAS cell lines. These protein will be candidate PATs for further studies. We also carried out qRT-PCR studies of the NRAS mutant cell line (SK-Mel30) and BRAF mutant cell line (A375) of all 23 DHHC-palmitoyl acyltransferases. We developed qRT-PCR probes that allow us to detect all of them effectively. From our studies, we have found that 5 DHHC genes are highly expressed in the NRAS mutant cell lines. By comparing the mass spec results and the mRNA profiling, we have narrowed down to 2 candidate genes which are highly enriched in NRAS mutant melanoma.

Task 1c. Carry out bioinformatics studies of the expression profiles in a large set of melanoma cell lines from previously published datasets (month 3-6).

Accomplishments: We carried out bioinformatics studies by data mining of public available expression profiles. From NCBI GEO data bases, we have identified melanoma expression profiles. We found that DHHC4 and DHHC5 are among the highly expressed PATs in NRAS mutant cells (**Figure 1**). These results support some of our findings using qRT-PCR methods described above, but not necessarily be the only methods to provide candidate PATs.

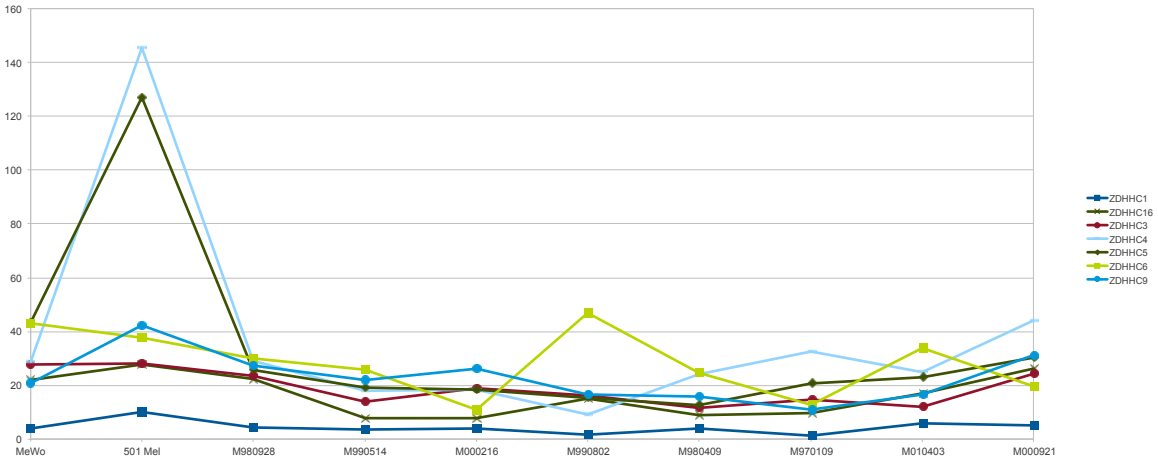

Figure 1. Bioinformatic analysis of melanoma samples using NCBI GEO dataset (GSE17349). The studies included NRas (G12D) mutant cell line (501Mel) confirmed by sequencing, and other melanoma cell lines and patient-derived samples. The expression data were analyzed across all ZDHHC-family proteins. ZDHHC4 and ZDHHC5 are highly expressed in NRas mutant melanoma cell line, but not in other cell lines.

Task 1d. Histology studies of PATs in melanoma cells to confirm that the protein levels of PATs are elevated in N-RAS mutant melanoma cell (month 6-12).

Accomplishments: We have studied the staining of a commercially available antibody for one of the top candidate PATs. However, this antibody did not recognize the correct protein in Western blot or immunoflurorescent staining. The antibody recognizes a different protein with a different size on the Western blot. The information showed on the vendor website is actually not correct. Therefore, there is no commercially available antibody could be used to study the protein level of the candidate PATs in histology. To address this issue, we will try to develop a new antibody that could recognize the protein. Alternatively, we will look at the expression level of the candidate PATs using data mining and bioinformatics methods as well as qRT-PCRs using primary tumor samples from a tissue array. This effort is on going and will likely to accomplished in the second year of the study.

Task2. To evaluate the effects of shRNAs targeting DHHC-PATs on NRAS activity, melanoma cell proliferation and apoptosis (Month 13-24):

We have carried out proposed work in Task 2 to evaluate the effects of DHHC-PATs in regulating NRAS signaling.

2a. We will co-transfect N-RAS and each of the candidate DHHC-PAT identified from ABPP in melanocytes or melanoma cells and evaluate whether any PATs can selectively activate N-RAS and drive N-RAS plasma membrane localization, and activation of downstream kinases (MEK, ERK etc.) by western blotting (month 13-15)

Accomplishments: Through proteomic studies, we previously found that DHHC5, DHHC17, DHHC18 and DHHC20 are the candidate PATs which showed elevated enzymatic activities in the NRAS mutant melanoma. To confirm with the chemical proteomic and expression profiling results in NRAS mutant melanoma cells, we first carried out qRT-PCR experiments to evaluate the expression levels of DHHC-PATs in NRAS mutant melanoma cells (Sk-Mel2 and Sk-Mel30), comparing with the non-NRAS mutant melanoma cells (501mel, IPC298 and A375). We have collected the total RNA samples from these cells and carried out qRT-PCR analysis using probes specific for each individual DHHC family members (23 of them). As shown in **Figure 2**, we found that DHHC3, DHHC6, DHHC13, and DHHC20 showed elevated the mRNA expressions in the NRAS mutant cells. Therefore, the mRNA expression level might not be correlating with the enzymatic activities.

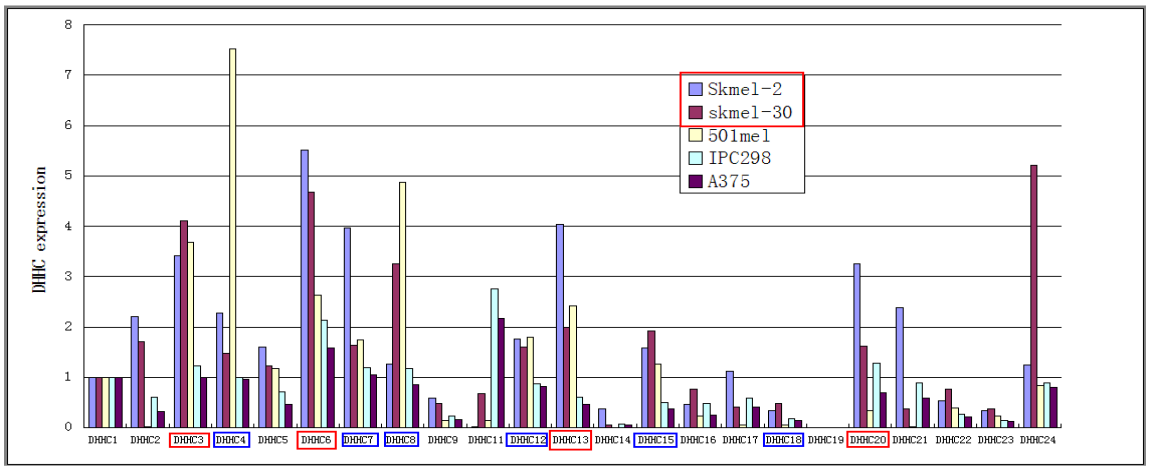

Figure 2. Quantitative RT-PCR examination of the mRNA expression levels of all DHHC-family PATs in melanoma cells. SK-Mel2 and Sk-Mel30 are the NRAS mutant melanoma cells.

Next, we transfected each individual PATs together with GFP-NRAS in cells to evaluate whether any of PATs can promote NRAS membrane localization. The mutant NRAS-GFP localized at cytoplasm (golgi or ER) and on the plasma membrane. Upon overexpress of different DHHC proteins, however, we could not detect significant change of their localization changes. Therefore, overexpression experiments are not sufficient to confirm which DHHC proteins are involved in NRAS regulation.

2b. knockdown the candidate DHHC-PATs in N-RAS mutant melanoma cells (Sk-Mel3, SK-Mel30, 501Mel etc.) using shRNAs (month 15-18).

1) generate cell lines with either stable knock-down and Tet-inducible knockdown of the protein of interest.

2) evaluate whether N-RAS oncogenic activity can be blocked (MEK, ERK phosphorylation, NRAS membrane localization) in these cell lines.

Accomplishments: We have cloned and generated lenti-viral shRNA constructs of all DHHC-PATs (4 shRNA sequences per gene). We selected DHHC5, DHHC13, DHHC17, DHHC18 and DHHC20 as candidate PATs in this experiment. We generated the lentivirals carrying the shRNA constructs and infected SK-mel30 cells with these virus.

We carried out puromycin selection to generate cells stably infected with the shRNAs. After 5-7 days of selection, we have successfully derived cell lines stably transfected with shRNAs. We next evaluated the shRNA knockdown efficiency using qRT-PCR, and have identified 1-2 shRNA constructs per gene which showed >60% of knock-down efficiency.

Next, we evaluated the localization of NRAS in these cells upon shRNA knock-down. We carried out immunoflurorescent staining of NRAS in these cells, and evaluated its localization under microscopy. Interestingly, we found that shRNA targeting DHHC5 is able to block NRAS membrane localization (**Figure 3**). Therefore, DHHC5 is a strong candidate of PAT that regulates NRAS activities in melanoma cells.

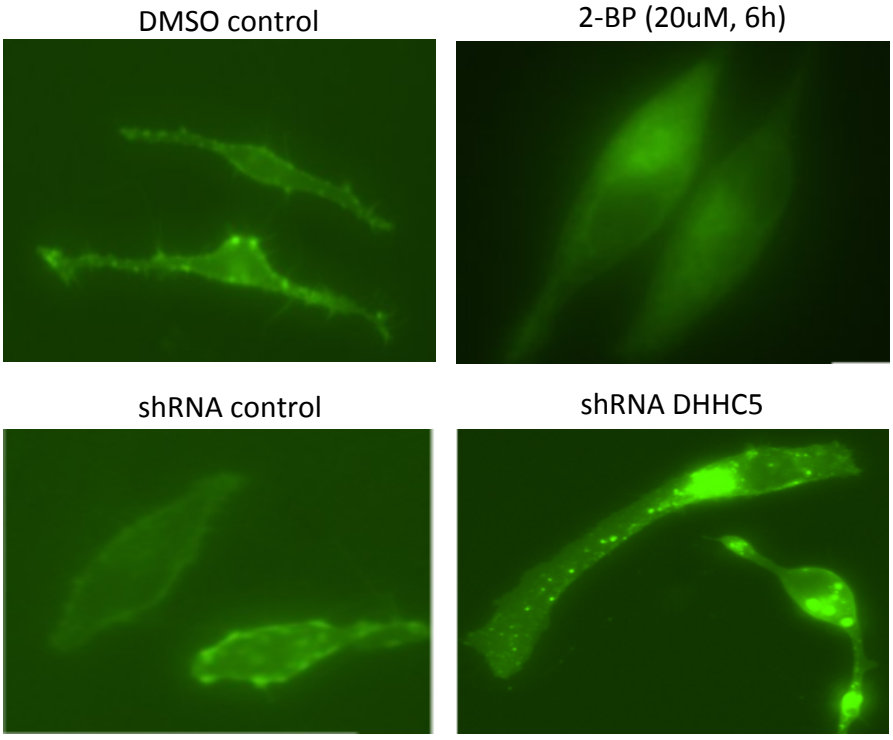

Figure 3. Imaging studies of NRAS membrane localization of Sk-Mel30 cells. Cells are treated with DMSO control or 2-bromopalmitate (2-BP) for 6h are evaluated under microscope. NRAS localized at the membrane in DMSO control treated cells. Treatment of palmitoyl acyltransferase inhibitor (2-BP) blocked NRAS membrane localization. Similarly, shRNA targeting DHHC5 can also block the membrane localization of NRAS in these cells.

In addition, we found that shRNA targeting DHHC13 also has some effects on blocking NRAS localization, although much weaker than DHHC5. It is possible that both DHHC5 and DHHC13 are involved in regulating NRAS localization in melanoma cells.

2c. knock-down the candidate PATs using shRNA in N-RAS melanoma cell lines to evaluate their effects on cell proliferation, colony formation and apoptosis in vitro (month 18-24).

Accomplishments: We have generated SK-mel-2 and Sk-mel30 cells with stably knockdown of DHHC5 and DHHC13. We have also generated DOX inducible

knockdown of DHHC5 and DHHC13 (the shRNA expression can be induced under doxycycline treatment). We have evaluated whether knocking down of these genes can block downstream signaling of mutant NRAS (p-Akt, p-MEK and p-ERK). We found that knocking down of DHHC5 and DHHC13 can indeed inhibit p-ERK levels in melanoma cells, suggesting that inhibiting DHHC proteins can block NRAS signaling (**Figure 4,5**).

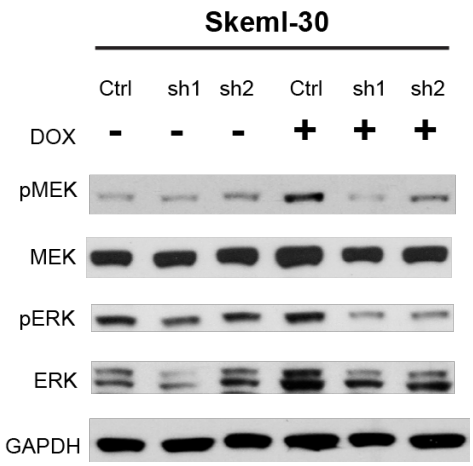

Figure 4. Knocking down of DHHC proteins affect NRAS signaling in melanoma cells. DOX inducible shRNA knocking down of DHHC13 can inhibit p-ERK levels in SK-mel-30 cells.

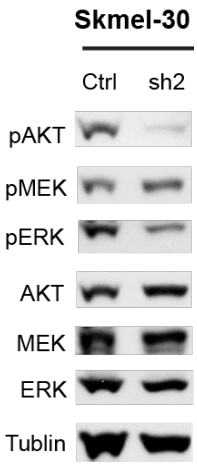

Figure 5. Knocking down of DHHC proteins affects p-AKT, p-MEK and p-ERK in melanoma cells. shRNA targeting DHHC5 can block p-AKT, p-MEK and p-ERK in SK-Mel30 cells.

We have tested the antiproliferation effects of shRNAs targeting the DHHC proteins. Our preliminary results suggest that knocking down either DHHC5 and DHHC13 can have only minor effects on proliferation. We will generate double-knock down of DHHC5 and 13 simultaneously, and to evaluate that inhibiting both DHHC proteins are required to block the proliferation of melanoma cells.

Task3. To design and synthesize analogues of cerulenin, a natural product inhibitor of palmitoyl acyltransferases to identify small molecule inhibitors of N-RAS palmitoylation. (in parallel with Task1 and 2, Month 0-24):

Task 3a. Synthesize compound libraries based on the structure of cerulenin. Modifications of their head and tail groups might improve their selectivity and potency. ~50 compounds will be synthesized in 0-12 month.

Accomplishments: We have designed cerulenin-based chemical probes to study palmitoyl acyltransferases. Cerulenin is a natural product inhibitor of fatty acid biosynthesis and protein palmitoylation. It has been shown that a palmitoyl analogue for cerulenin has good selectivity over fatty acid synthases. We have synthesized an alkyne analogue of cerulenin and a synthetic strategy has been developed (**Figure 6**).

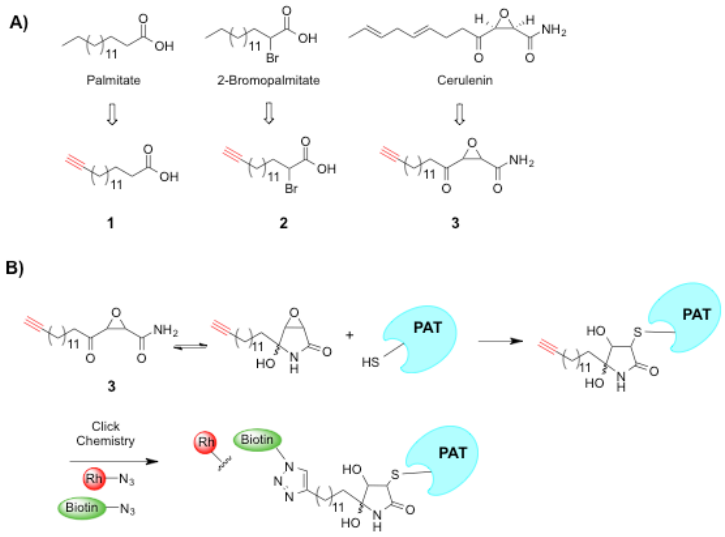

Figure 6. Design of Cerulenin-based chemical probes. (A) structures of the substrate labeling probe **1**, PATs activity probe **2** based on 2-bromopalmitate and probe **3** based on cerulenin. (B) Labeling and detection of palmitoyl acyltransferases by probe **3**. Figure adapted from our publication: Zheng et al. ACS Chem. Biol. 2015.

Using the synthetic route that we developed in this task, we have synthesized several analogues of cerulenin with variations at the head groups. We have finished synthesis of 10 analogues, and will test their effects in melanoma cells.

What opportunities for training and professional development have the project provided?

The PI has strong background in chemistry and drug discovery. His career goal is to become a leading scientist and independent investigator in melanoma and skin cancer drug discovery. To achieve the career goal, the mentor (Dr. Fisher) has been guiding Dr. Wu's melanoma research through routine meetings and discussions. Dr. Wu has participated the MGH melanoma program weekly meeting chaired by Dr. Fisher. Dr. Wu has attended the melanoma workshops sponsored by Dana-Farber/Harvard Cancer Center (DF/HCC) and the Koch Institute of Cancer Research at MIT, which was organized by Dr. Fisher. These workshops covered melanoma clinical trials studies, melanoma genomics and drug discovery, and will provide additional training and collaboration opportunities for young investigators. Dr. Wu has participated the melanoma journal club and seminars in MGH and Harvard community, where he will learn the progresses in melanoma research.

How were the results disseminated to communities of interest?

Nothing to report.

4. IMPACT

What was the impact on the development of the principle discipline of the project?

We have demonstrated that a chemical approach using Activity based protein profiling (ABPP) could study the palmitoyl acyltransferases in melanoma. We have developed multiple chemical tools to study PATs in cancer cells. Our study has identified candidate PATs possibly as new therapeutic targets, which could have significant impact in drug discovery and cancer research.

What was the impact on other disciplines?

Nothing to report

What was the impact on technology transfer?

Nothing to report

What was the impact on society beyond science and technology?

Nothing to report

5. CHNAGES/PROBLEMS

Changes in approach and reasons for change:

Our results have shown that single knock-down of DHHC5 or DHHC13 could inhibit downstream NRAS signaling. However, knocking down DHHC5 or DHHC13 alone has only minor impact on the cell proliferation. It is likely that we need to knockdown both DHHC5 and DHHC13 at the same time to achieve the anticancer effects. We will generate cells with stably knocking down of both DHHC proteins to test the hypothesis.

6. PRODCUTS

Publications: Manuscripts describing the work have been published. The PDF files of have been included in this report.

"A Clickable Analogue of Cerulenin as Chemical Probe to Explore Protein Palmitoylation" Baohui Zheng, Shunying Zhu, and Xu Wu*, ***ACS chemical biology***, 2015 Jan 16;10(1):115-21. doi: 10.1021/cb500758s. Epub 2014 Oct 23.

"Autopalmitoylation of TEAD Proteins Regulates Transcriptional Output of the Hippo Pathway" PuiYee Chan, Xiao Han, Baohui Zheng, Michael DeRan, Jianzhong Yu,

Gopala K. Jarugumilli, Hua Deng, Duojia Pan, Xuelian Luo * and Xu Wu* ***Nature Chemical Biology***, 2016, Published online: Feb. 22nd, doi: 10.1038/nchembio.2036

(This work is not directly related to this funding, however, the probes made under this grant have been used in this paper, and we have acknowledged this funding).

Acknowledgement of federal support: Yes

Other products:

Research material: chemical probes for palmitoyl acyltransferases (16C-BYA and 16-EYA)

7. PARTICIPANTS & OTHER COLLABORATING ORGANIZATIONS

What individuals have worked on the project?

Name:	Xu Wu
Project Role:	PI
Researcher Identifier (e.g. ORCID ID):	0000-0002-1624-0143
Nearest person month worked:	3
Contribution to project:	Dr. Wu has supervised the research, designed the experiments and interpreted the results
Funding support:	MGH Institutional fund American Cancer Society Melanoma Research Alliance National Cancer Institute

Name:	Baohui Zheng
Project Role:	Research Fellow
Researcher Identifier (e.g. ORCID ID):	N/A
Nearest person month worked:	6
Contribution to project:	Dr. Zheng has performed work in the area of synthesis,

	chemical labeling and mass spectrometry
Funding support:	Melanoma Research Alliance

Name:	Michael DeRan
Project Role:	Research Fellow
Researcher Identifier (e.g. ORCID ID):	N/A
Nearest person month worked:	3
Contribution to project:	Dr. DeRan has performed work in the area of biochemistry, and mRNA expression profiling
Funding support:	MGH Institutional fund American Cancer Society National Cancer Institute

Has there been a change in the active other support of the PD/PI(s)?

During the funding period, the PI has been awarded 2 NIH R01 grants.

National Cancer Institute (NCI)/NIH, Wu (PI)

1R01CA187909-01

Metabolic regulation of cellular tight junction proteins

The goal of this proposal is to study the regulation of cellular junction proteins AMOTL1 by AMPK, and whether this regulation lead to inhibition of YAP oncogene in cancers in vitro and in vivo.

Overlap: None

This award will not impact the level of efforts for the DoD grant.

National Institute of Diabetes and Digestive and Kidney Diseases (NIDDK)/NIH, Wu (PI)
R01DK107651-01

Chemical approach to study autopalmitoylation of transcription factors

The major goals of this project are to investigate the regulations, mechanisms, and functions of TEAD transcription factor autopalmitoylation using activity-based chemical probes, and to develop small molecule inhibitors of TEADs.

Overlap: None

This award will not impact the level of efforts for the DoD grant.

What other organizations were involved as partners?

Nothing to report.

8. SPECIAL REPORTING REQUIREMENT

N/A

9. APPENDICES

Yes.

PDF files of the publications.

ACS chemical biology

Letters

pubs.acs.org/acschemicalbiology

Clickable Analogue of Cerulenin as Chemical Probe to Explore Protein Palmitoylation

Baohui Zheng, Shunying Zhu, and Xu Wu*

Cutaneous Biology Research Center, Massachusetts General Hospital, Harvard Medical School, Building 149, 13th Street, Charlestown, Massachusetts 02129, United States

Supporting Information

ABSTRACT: Dynamic palmitoylation is an important post-translational modification regulating protein localization, trafficking, and signaling activities. The Asp-His-His-Cys (DHHC) domain containing enzymes are evolutionarily conserved palmitoyl acyltransferases (PATs) mediating diverse protein S-palmitoylation. Cerulenin is a natural product inhibitor of fatty acid biosynthesis and protein palmitoylation, through irreversible alkylation of the cysteine residues in the enzymes. Here, we report the synthesis and characterization of a "clickable" and long alkyl chain analogue of cerulenin as a chemical probe to investigate its cellular targets and to label and profile PATs *in vitro* and in live cells. Our results showed that the probe could stably label the DHHC-family PATs and enable mass spectrometry studies of PATs and other target proteins in the cellular proteome. Such probe provides a new chemical tool to dissect the functions of palmitoylating enzymes in cell signaling and diseases and reveals new cellular targets of the natural product cerulenin.

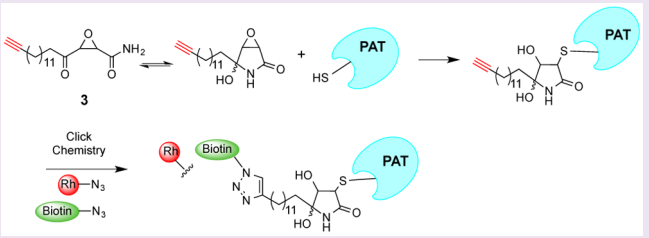

Protein S-palmitoylation is the post-translational attachment of the 16-carbon palmitate to the cysteine residues of proteins through a thioester linkage.[1,2] In contrast to other lipid modifications of proteins, S-palmitoylation is a dynamic process. In response to extracellular or intracellular signals, the palmitoylation−depalmitoylation process precisely regulates the localization, trafficking, and cofactor binding properties of proteins.[3] A large number of palmitoylated proteins have been identified by biochemical and proteomic methods.[4−7] Palmitoylation is essential for the signaling functions of Src-family kinases, Ras GTPase, G-proteins, G-protein coupled receptors (GPCRs), and synaptic adhesion molecules.[8] For example, palmitoylation of the two C-terminal cysteine residues is required for the proper trafficking and membrane localization of H-Ras and N-Ras.[9] Disrupting the palmitoylation and depalmitoylation cycle could effectively block their oncogenic functions, suggesting that targeting protein palmitoylation could provide potential therapeutic options for diseases.[10] Therefore, it is important to develop chemical tools to dissect the functions of palmitoylation in signaling and diseases.

Protein S-palmitoylation can be mediated by nonenzymatic or enzymatic processes.[1] Some proteins bind to palmitoyl-Coenzyme A (CoA) directly, resulting in thioester exchange reactions with the proximal cysteine residues in the proteins.[11] For example, purified Gα protein could be autopalmitoylated when incubated with palmitoyl-CoA.[12] Therefore, the concentration of cellular palmitoyl-CoA pool could greatly influence the level of autopalmitoylation. Yeast genetic studies have revealed that enzymatic palmitoylation involves a family of highly conserved protein palmitoyl acyltransferases (PATs).[13,14] These enzymes are generally transmembrane proteins with a conserved Asp-His-His-Cys (DHHC) domain in the active site. The human genome encodes 23 DHHC-family PATs. These enzymes are usually localized in the ER, Golgi, or at the plasma membrane of cells and regulate the palmitoylation of diverse protein substrates. Genetic and biochemical studies have provided insights to the functions of many DHHC enzymes and their substrates.[15] For example, mice with a loss-of-function mutation of DHHC13 showed multiple aging related phenotypes, including alopecia, osteoporosis, systemic amyloidosis, and early death.[16] The *dhhc17*$^{-/-}$ mice display neurodegenerative phenotypes, highlighting the function of DHHC17 in regulation of synaptic and neuronal functions.[17] A point mutation in DHHC21 was identified in the *depilated* (*dep*) mouse mutant, resulting in hair follicle degeneration.[18] Furthermore, DHHC9, 11, 14, and 17 proteins are shown to be deregulated in bladder, lung, and colon cancers and in leukemia and could contribute to oncogenic processes.[19−21] In addition to the S-palmitoylation, membrane-bound O-acyltransferases (MBOAT) such as Porcupine and Hedgehog acyltransferase (Hhat) could mediate the O- and N-palmitoylation of Wnt and Hedgehog proteins, respectively.[22,23] Interestingly, acyltransferases, which were previously unrecognized as PATs, might catalyze protein palmitoylation. For example, lysophosphatidylcholine acyltransferase 1 (Lpcat1) has been reported to mediate the O-

Special Issue: Post-Translational Modifications

Received: July 3, 2014
Accepted: October 16, 2014
Published: October 16, 2014

DOI: 10.1021/cb500758s
ACS Chem. Biol. 2015, 10, 115−121

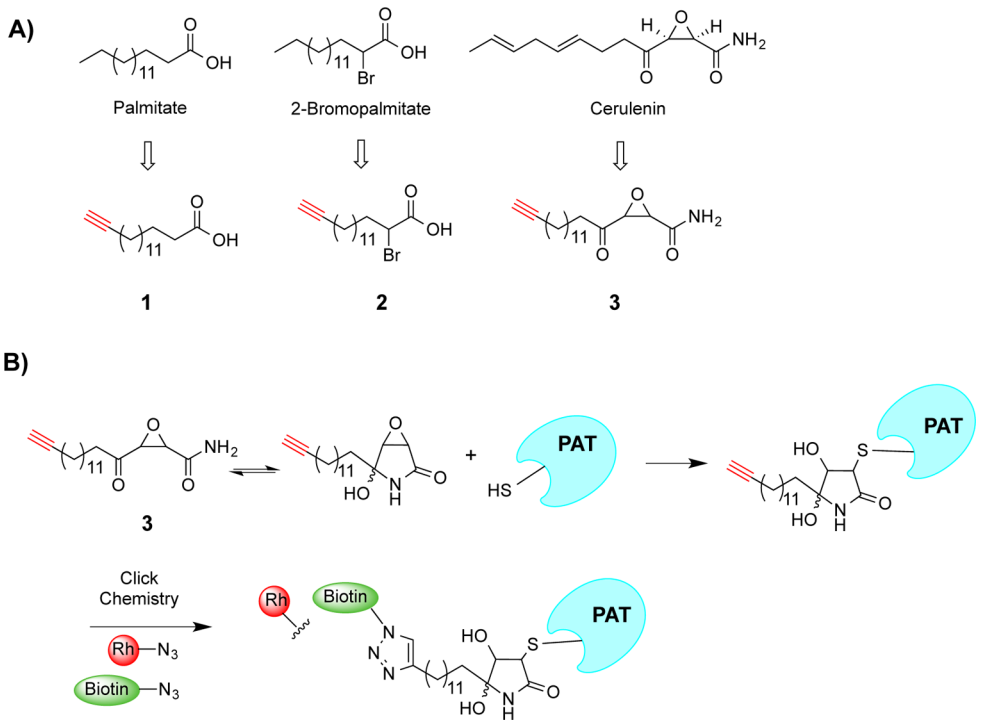

Figure 1. Chemical probes to study protein palmitoylation. (A) Structures of the substrate labeling probe **1**, PATs activity probe **2** based on 2-bromopalmitate, and probe **3** based on cerulenin. (B) Labeling and detection of palmitoyl acyltransferases by probe **3**.

palmitoylation of histone H4 protein.[24] These reports highlight the importance of identifying new palmitoylating enzymes or autoacylating proteins and revealing their functions in signaling and diseases.

To profile and study palmitoylation, analogues of palmitate, such as 15-hexadecynoic acid (**1**), have been widely used as chemical probes to metabolically label palmitoylated proteins (substrates).[25] We sought to develop chemical probes to covalently label and profile PATs (enzymes) to elucidate their functions in signal transduction. Previously, we have reported the activity-based protein profiling (ABPP) probe (**2**) for PATs, based on the irreversible and pan-inhibitor 2-bromopalmitate (2-BP) (Figure 1A).[26] Probe **2** (20−100 μM) could effectively label PATs in live cells, but not in cell lysates *in vitro*, suggesting that metabolic conversion to its CoA derivatives might significantly enhance its activity. We used probe **2** to label and profile endogenous palmitoyl acyltransferases in cells and have identified many acyltransferases and palmitoylated proteins, suggesting that **2** could also be incorporated into the cellular lipid pool and utilized as an acyl donor. To improve the efficiency and specificity of the labeling, we sought to synthesize and characterize new chemical probes for PATs and autopalmitoylated proteins.

The natural product cerulenin ([2*R*,3*S*]-2,3-epoxy-4-oxo-7,10-*trans*,*trans*-dodecadienoylamide) has been studied as an antifungal and antibacterial agent for nearly 30 years and known to inhibit fatty acid synthesis and protein palmitoylation.[27] The structure of cerulenin is composed of an α-keto-epoxycarboxamide with an octadienyl side chain. It exists in an equilibrium between the open chain and a cyclized hydroxylactam form. The epoxycarboxamide moiety has been proposed as the "warhead" of the compound, which alkylates the cysteine residues in fatty acid synthase and palmitoyl acyltransferases, leading to irreversible inhibition.[28] We recently found that cerulenin can compete with probe **2** in labeling of DHHC domain containing PATs, suggesting that it might occupy the same or an adjacent binding site of acyl-CoA and inhibit the acyl-enzyme adduct formation.[26] Previously, the structure−activity relationship (SAR) studies of ∼30 cerulenin analogues have shown that the α-keto-epoxide moiety is essential for the palmitoylation inhibition activity.[29] Interestingly, analogues with a long saturated aliphatic chain (15−17 carbon chain) showed improved potency in inhibiting H-Ras and N-Ras palmitoylation, while not inhibiting fatty acid synthesis.[29] On the basis of these reports, we hypothesized that a "clickable" long aliphatic chain analogue of cerulenin might serve as a chemical probe to directly label palmitoylating enzymes, allowing proteomic and imaging studies of palmitoyl acyltransferases *in vitro* and in cells (Figure 1B).

Toward this end, we synthesized the cerulenin analogue **3** (cis-2,3-epoxy-4-oxooctadec-17-ynamide) as a chemical probe for palmitoylating enzymes (Figure 1B). The synthesis of **3** was achieved as illustrated in Scheme S1 in Supporting Information, modified from previously reported methods.[30] Notably, the key intermediate γ-lactone was synthesized through selenolactonization to introduce the terminal alkyne. Specifically, (*E*)-octadec-3-en-17-ynoic acid was added to PhSeCl solution with Et_3N in CH_2Cl_2 at −78 °C. The mixture was warmed to −40 °C over 40 min to afford the intermediate, which was then oxidized by 35% of H_2O_2 for 40 min. The desired product octadec-2-en-17-ynoic acid γ-lactone can be synthesized with good yield (50%). The final product **3** can be readily made with 15% of overall yield. The detailed synthetic procedures and compound characterization are described in the Supporting Information.

We set out to test whether probe **3** could label exogenous PATs in cells first. We transfected HEK293 cells with expression vectors carrying hemagglutinin (HA)-tagged mouse DHHC4. Forty-eight hours after transfections, we treated the cells with various concentrations of probe **3** (0.5 to

DOI: 10.1021/cb500758s
ACS Chem. Biol. 2015, 10, 115−121

10 μM) and incubated for 5 h. We isolate the cell lysates and subsequently carried out Cu-mediated 1,3-dipolar cycloaddition (Click reaction) with biotin-azide. The labeling efficiency was evaluated by streptavidin blot. As shown in Figure 2A, we could

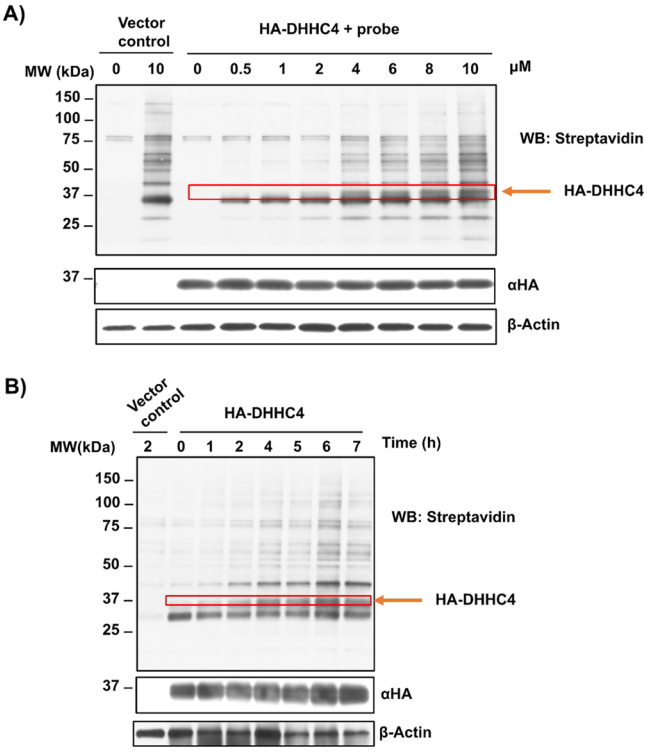

Figure 2. Cerulenin analogue **3** labeled HA-tagged DHHC4 protein in HEK293 cells. (A) HEK293 cells transfected with vector control or HA-DHHC4 expression vector were treated with different concentrations of probe 3 for 5 h. The labeling of DHHC4 was detected by Click chemistry using biotin azide followed by streptavidin blot. The expression of DHHC4 was confirmed by Western blot using anti-HA antibody. (B) HEK293 cell transfected with vector control or HA-DHHC4 were treated with 10 μM of probe **3** for the indicated time.

detect the labeling of DHHC4 by probe **3** at concentrations as low as 2 μM, consistent with reported cellular activity of cerulenin in inhibition of palmitoylation. Probe **3** appeared to be more potent than previously reported 2-BP-based probe **2**, which effectively labeled DHHC4 proteins at concentrations around 50−100 μM. The improved potency of labeling might be resulted from the stronger chemical reactivity of the epoxide warhead in the probe. We then tested the time dependency of the labeling. Similarly, we transfected cells with HA-DHHC4 expression vector, and then treated cells with **3** at 10 μM. We isolated the cell lysate at various time points (1 to 7 h), followed up with Click chemistry with biotin-azide and Western blotting. We observed that probe **3** could label exogenous DHHC4 after 1 h of incubation. The labeling efficiency increased with longer incubation time and peaked after 4−6 h of incubation (Figure 2B). Overall, probe **3** has better efficiency and potency to label DHHC4 protein in cells, compared to our preciously reported probe **2**.

It is known that 2-BP and probe **2** could be metabolically converted to the Coenzyme A (CoA) derivatives in live cells, and the CoA derivatives are much more potent and effective to alkylate DHHC4. Such properties might limit the *in vitro* application of probe **2**, such as in enzyme-based high throughput assays, where purified enzymes in cell-free systems are preferred. In contrast, cerulenin might directly alkylate the protein by epoxide ring opening reactions *in vitro*, thus metabolic conversion in live cells are not required for its labeling activity. We isolated cell lysates from HEK293 cells expressing HA-DHHC4 using nondenaturing conditions and tested whether probe **3** could directly label PATs *in vitro* in cell lysates. We treated cell lysate or heat-inactivated lysate with probe **3** for 5 h. We immunoprecipitated HA-tagged DHHC4 with anti-HA antibody and then proceeded to perform the Click reaction with biotin-azide. The active DHHC4 enzyme in the lysate could be labeled, while heat-inactivated DHHC4 could not, suggesting that **3** could label native DHHC4 protein, but not the denatured enzyme *in vitro* (Figure 3A). In addition, the labeling required PATs in their native, nondenatured state, suggesting the labeling might not be a result of nonspecific alkylating of cysteine residues in the proteins, but rather through binding and alkylating specific residues around the binding site.

15-Hexadecynoic acid (**1**), the 16-carbon fatty acid with terminal alkyne group, has been widely used as a reporter of palmitoylated proteins.[25] It mimics palmitate and forms a labile thioester linkage with the substrate proteins, which can be removed by treatment with 2.5% hydroxylamine (NH_2OH). It labels DHHC-family PATs by forming an acyl-enzyme intermediate or labels the peripheral palmitoylation sites of PATs.[31] However, treatment of hydroxylamine readily removed the thioester adduct formed by **1** and DHHC4. As cerulenin alkylates DHHC proteins by epoxide ring opening, it should form a stable adduct with the enzyme. We treated HEK293 cells expressing HA-DHHC4 with probes **1** and **3** for 5 h, and the cell lysates were subsequently treated with or without 2.5% hydroxylamine for 5 min. We evaluated the probe labeling by Click chemistry with biotin-azide and streptavidin blot. Indeed, cerulenin-based probe **3** forms a hydroxylamine-resistant stable adduct with DHHC4 protein, where the control probe **1** forms labile adduct with the enzyme (Figure 3B). This result is consistent with the proposed mechanism that probe **3** could directly alkylate the enzyme.

The DHHC family of PATs contain a cysteine-rich domain including the Asp-His-His-Cys (DHHC) catalytic motif. Mutations of the cysteine in the DHHC motif to serine or alanine residues abolished the acyl transferase activity and prevented enzyme autoacylation.[32] Previously, we have shown that the 2-BP-based probe **2** labels the wild-type enzyme but not the catalytically inactive mutant enzymes, suggesting that **2** is an activity-based probe for PATs and the conserved cysteine residue in the DHHC motif might be the site of labeling.[26] To test whether the cerulenin analogue **3** has similar labeling activity, we transfected cells with HA-tagged wild-type DHHC3 and 4 or their mutants (DHHC3, C157S and C157A; DHHC4, C179S and C179A, respectively), where the conserved cysteine residues in the DHHC motif were mutated to serine or alanine residues. Interestingly, 10 μM **3** effectively labeled not only the wild-type proteins but also the mutants. These results strongly suggest that cerulenin or its analogue **3** alkylates other cysteine residues proximal to its binding site (Figure 3C), and the core cysteine residue at the DHHC motif might not be the sites of alkylating. Moreover, as the enzymatically inactive proteins can still be labeled, probe **3** would not be characterized as an activity-based probe, but rather a reactive chemical probe that could bind to and alkylate PATs. These results also confirmed previous speculation that cerulenin and probe **3** are not a

DOI: 10.1021/cb500758s
ACS Chem. Biol. 2015, 10, 115−121

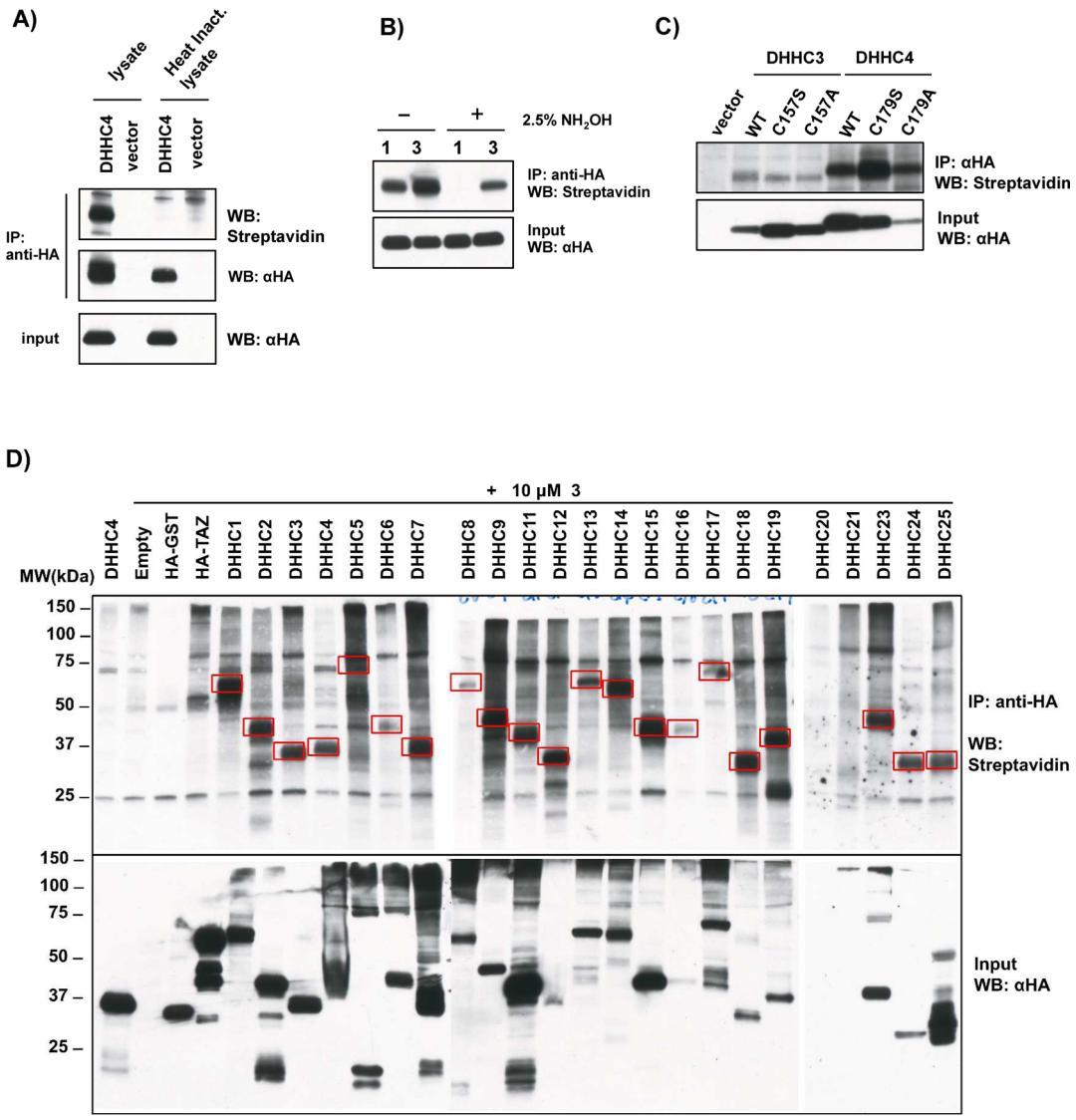

Figure 3. (A) Ten micromolar probe **3** could label DHHC4 *in vitro* in cell lysates, but not in heat-inactivated lysate. (B) Probe **3** stably labeled DHHC4 and formed hydroxylamine-resistant adduct, whereas probe **1** forms a labile thioester intermediate with the enzyme. (C) Mutations of cysteine residue at the DHHC domain in DHHC3 and 4 do not disrupt the labeling of probe **3**. (D) Probe **3** labeled DHHC family of palmitoyl acyltransferases. The red boxes indicated the labeled DHHC proteins based on their molecular weight and positions in the anti-HA Western blot.

mechanism-based irreversible inhibitor of PATs and mechanistically different from 2-BP and probe **2**, offering different labeling tools for PATs. Several disease relevant mutations in DHHC proteins might disrupt their catalytic activities, such as the loss-of-function mutation of DHHC13 in the systemic amyloidosis mouse model. Such mutant PATs could be labeled by probe **3** but not probe **2**. Profiling the samples with these two probes in parallel could provide an approach to study the abundance of catalytically defected vs catalytically active PATs in these disease-relevant models.

As described previously, although 2-BP based probes could label most DHHC-PATs tested, they failed to label several important PATs, including DHHC1, 8, and 23.[26,33] To evaluate whether cerulenin-based probe **3** could have better generality and versatility in labeling members of DHHC-family PATs, we expressed all 23 HA-tagged DHHCs in HEK293 cells and carried out labeling experiments with 10 μM **3** for 5 h. We immunoprecipitated the DHHC proteins using anti-HA antibodies and carried out the Click reaction with biotin-azide. The streptavidin blot in Figure 3D shows that all of the expressed PATs could be successfully labeled with **3**. DHHC20 and DHHC21 were poorly expressed in HEK293 cells and have relatively weak labeling. We observed that the intensity of the labeling largely correlates with the expression levels of the proteins in the lysates. However, probe **3** has higher labeling efficiency for DHHC12 and DHHC18 but weaker efficiency for DHHC6 and DHHC8. Such differences in labeling activity might be resulted from the differences in binding affinity of the probe toward different DHHC-PATs or the reactivity of the proximal cysteine residues in the proteins. Nevertheless, DHHC1, 8, and 23 could be successfully labeled by **3**, suggesting that probe **3** offers broader coverage of the DHHC family of PATs compared with previously reported probes. Taken together, we have shown that the probe **3** could be used as a chemical probe to label and profile the DHHC-family PATs and is superior to previously reported probes with broader labeling activity and higher potency.

DOI: 10.1021/cb500758s
ACS Chem. Biol. 2015, 10, 115–121

Table 1. Representative Proteins Labeled by Probe 3 and Could Be Competed off by 2-BP and Cerulenin[a]

symbol	protein name	DMSO	probe 3	probe 3 + 2BP	probe 3 + cerulenin
RTN4	reticulon-4	4	164	74	78
VDAC2	voltage-dependent anion-selective channel protein 2	11	140	30	40
FABP5	fatty acid-binding protein, epidermal	4	103	1	9
VDAC3	voltage-dependent anion-selective channel protein 3	3	101	48	49
HMOX2	heme oxygenase	1	100	43	45
ATP2A2	sarcoplasmic/endoplasmic reticulum calcium ATPase 2	6	94	30	54
CYB5B	cytochrome b5 type B	3	63	17	18
ATP2A1	sarcoplasmic/endoplasmic reticulum calcium ATPase 1	5	61	29	38
HM13	minor histocompatibility antigen H13	0	55	21	16
SEC63	translocation protein SEC63 homologue	0	38	4	5
TXNDC5	thioredoxin domain-containing protein 5	6	38	20	11
TRAPPC3	trafficking protein particle complex subunit 3	0	36	2	5
ENDOD1	endonuclease domain-containing 1 protein	0	35	5	6
MTAP	*S*-methyl-5′-thioadenosine phosphorylase	0	34	11	16
HCCS	cytochrome c-type heme lyase	0	33	8	7
APOL2	apolipoprotein L2	0	32	7	9
TMX1	thioredoxin-related transmembrane protein 1	0	31	18	17
MLANA	melanoma antigen recognized by T-cells 1	3	28	4	7
BACH1	transcription regulator protein BACH1	0	27	2	4
CD81	CD81 antigen	4	25	5	5
LPCAT2	lysophosphatidylcholine acyltransferase 2	0	25	2	4
COMT	catechol O-methyltransferase	2	24	16	8
HEATR3	HEAT repeat-containing protein 3	0	21	6	1
ZDHHC20	probable palmitoyltransferase ZDHHC20	0	19	4	7
AP1AR	AP-1 complex-associated regulatory protein	0	16	2	0
GLTP	glycolipid transfer protein	0	13	1	0
ALG6	dolichyl pyrophosphate Man9GlcNAc2 alpha-1,3-glucosyltransferase	0	12	1	0
MIEN1	migration and invasion enhancer 1	0	12	0	0
UBR7	Putative E3 ubiquitin-protein ligase UBR7	0	11	0	0
LPCAT1	Lysophosphatidylcholine acyltransferase 1	0	9	1	2
ST6GALNAC3	alpha-*N*-acetylgalactosaminide alpha-2,6-sialyltransferase 3	0	9	0	0
RABGGTB	geranylgeranyl transferase type-2 subunit beta	0	8	0	1
C18orf32	UPF0729 protein C18orf32	0	7	0	1
VKORC1	vitamin K epoxide reductase complex subunit 1	0	5	0	0
EPT1	Ethanolaminephosphotransferase 1	0	4	0	0

[a]The number of total matched peptide spectra of representative acyltransferases, PATs, and other abundant proteins is listed. The full list of identified proteins can be found in the Supporting Information.

To identify the cellular targets of the cerulenin analogue **3**, we carried out labeling experiments in 501Mel melanoma cells with 10 μM **3** for 5 h. The cell lysates were then subjected to Click chemistry using biotin-azide and enriched by streptavidin beads. The labeled proteins were digested on beads by trypsin and analyzed by mass spectrometry. We filtered the mass spectrometry results for proteins with >2 spectra counts in duplicate and with >5-fold enrichment over the DMSO control samples. We have identified >200 total proteins as putative cellular targets of probe **3**, suggesting that the cerulenin analogue could alkylate diverse proteins in cells (Table 1 and Supplementary Table 1). Among them, we have identified endogenous palmitoyl acyltransferase ZDHHC20. ZDHHC5, ZDHHC4, and ZDHHC6 were also identified by mass spectrometry from these cells but did not pass the stringent threshold. Many other acyltransferases and acyl-CoA binding enzymes were also labeled by **3**, including lysophosphatidylcholine acyltransferase 1 (LPCAT1), which is reported as O-palmitoylation enzyme for histone H4; and MBOAT7, a member of membrane-bound acyltranferases. The most abundant targets enriched by probe **3** include reticulon 4 (RTN4), heme oxygenase 2 (HMOX2), voltage-dependent anion channels (VDAC2 and VDAC3), and ER calcium ATPase (ATP2A2). Interestingly, these proteins are also targets of the 2-BP based probes, suggesting that these two probes have some overlapping cellular targets. However, several proteins, which are labeled by 2-BP probes, including carnitine O-palmitoylacyltransferase (CPT1), were not among the proteins identified by probe **3**, suggesting that these probes have different labeling specificity toward certain acyltransferases. Several common targets, such as reticulon, cytochrome b5, FLOT2, and ESYT2 are also known as palmitoylated proteins (substrates). As cerulenin and 2-BP could inhibit PATs activities in cells, it is interesting to further study whether these common targets were palmitoylated through nonenzymatic processes or palmitoylated by PATs, which were not inhibited by 2-BP and cerulenin. More importantly, we observed several proteins, which are uniquely labeled by probe **3**. For example, probe **3** could label acyl protein thioesterase 1 (APT1/LYPLA1), which is the enzyme responsible for depalmitoylation. Furthermore, we did not identify fatty acid synthase complex proteins from the mass spectrometry studies, consistent with the notion that the long alkyl chain analogue

DOI: 10.1021/cb500758s
ACS Chem. Biol. 2015, 10, 115−121

of cerulenin specifically inhibits palmitoylation but not fatty acid synthase.

To further reveal whether the protein targets labeled by probe **3** are common targets of cerulenin and 2-BP involved in palmitoylation, or cerulenin or probe **3** specific targets, we carry out competition labeling and mass spectrometry studies of probe **3**. We pretreated 501Mel cells with 2-BP (100 μM) or cerulenin (10 μM) for 4 h, and then added probe **3** (5 μM) to the cells. We isolated the cell lysates after 4 h of probe incubation and carried out Click chemistry with biotin-azide as described previously. We observed that certain bands are indeed competed off by 2-BP and cerulenin (Supplementary Figure S1). To reveal the identities of common target proteins of 2-BP, cerulenin and probe **3**, and protein targets that are specific for cerulenin, we enriched the labeled proteome using streptavidin beads and then carried out on-beads digestion by trypsin and then analyzed the proteins by mass spectrometry. We observed that ~140 proteins, which can be competed off by 2-BP and cerulenin (with >2-fold less total peptide spectra counts in the presence of competitors), suggesting that these proteins are common targets of these two palmitoylation inhibitors and probe **3**. These common targets include the known palmitoylated protein or PATs, such as reticulon 4, VDAC2, ZDHHC20, and LPCAT1. Interestingly, we also observed that ~15 proteins can be competed off by cerulenin, but not 2-BP. These proteins, including thioredoxin reductase 1 (TXNRD1), exportin 1 (XPO1), and GPR143, might represent protein target specific for cerulenin and probe **3**, which should have different reactivity and specificity than 2-BP and might label proteins not involved in palmitoylation. Furthermore, we have observed several proteins that can be competed off by 2-BP, but not cerulenin, including cholesterol ester hydrolase 1 (NCEH1), PML protein, and acyl protein thioesterase (LYPLA1/APT1). As the long alkyl chain moiety in probe **3** could improve its specificity toward palmitoylating proteins compared to cerulenin, these targets might represent palmitoylated proteins that cerulenin could not label. In summary, we could evaluate whether the proteins are cerulenin-specific targets or palmitoylation-related targets by competition assays.

To assess whether our methods could identify novel palmitoylated/palmitoylating proteins, we chose to validate whether lysophosphatidylcholine acyltransferase 2 (LPCAT2) and acyl protein thioesterase (LYPLA1/APT1) are indeed palmitoylated. We labeled the proteome of 501Mel cells for 8 h using the 15-hexadecynoic acid (**1**), which has been widely used as a reporter of palmitoylated proteins.[25] We then carried out Click chemistry using biotin-azide and immunoprecipitated the palmitoylated proteins using streptavidin beads. The bounded proteins were eluded using biotin-containing buffer. We then used anti-LPCAT2 or anti-LYPLA1 antibodies in Western blot. We have successfully detected that endogenous LPCAT2 and LYPLA1/APT1 are indeed palmitoylated (Supplementary Figure S2). A recent report suggested that APT1 palmitoylation might be involved in its localization at the Golgi apparatus.[34] Therefore, palmitoylation of APT1 could play important roles in regulating its biological functions. Further studies are needed to elucidate the detailed functions of palmitoylation in regulation of LPCAT2 and APT1.

Taken together, here we report synthesis and characterization of a novel chemical probe for protein palmitoylation and palmitoyl acyltransferases. Compared to previously reported PATs probes, probe **3** has several advantages. It has an improved potency and could be used at much lower concentration *in vitro* and in cell culture. In addition, probe **3** does not require metabolic conversion in live cells and thus can directly label PATs *in vitro*. This feature allows its applications in enzymatic assays or developing cell-free assays for high throughput screening. More importantly, it labeled all the DHHC-PAT family members we have tested, suggesting it is a much broader and more universal chemical probe to profile PATs. We also successfully enriched the cellular targets of this probe and identified endogenous PATs and thioesterase from the proteome. Therefore, it could be used as a chemical probe to facilitate the identification of additional palmitoylating enzymes and autoacylated proteins involved in signaling and diseases. From our mass spectrometry studies, we found that probe **3** could also label proteins that are not previously known to be involved in palmitoylation. These proteins could be the new cellular targets of cerulenin. This is not surprising for irreversible chemical probes, which often target multiple proteins of different classes. For example, an alkyne-aspirin probe has been shown to label more than 120 proteins, and a majority of them were not previously identified as targets of aspirin.[35] Nevertheless, such covalent probes significantly expand our knowledge of new cellular targets of known drugs and natural products, and such polypharmacological effects might be the underlying mode-of-action of these compounds. Previously, epoxide containing oxirane probes were also reported to explore antibiotic targets in bacteria.[36] The long alkyl chain of cerulenin is a unique structural feature, which improves its specificity toward lipid binding and palmitoylating proteins in mammalian cells. This feature distinguishes it from a generic "epoxide" chemical probe, which might nonspecifically alkylate many cellular proteins. In summary, the clickable analogue of cerulenin represents a new chemical probe to explore palmitoylation and PATs in signal transduction. Further investigation of the functions of the identified target proteins could reveal new insights to this important posttranslational modification.

METHODS

Material, synthetic procedures, and labeling methods are described in the Supporting Information.

ASSOCIATED CONTENT

Supporting Information

Synthesis, experimental protocols, full list of identified proteins from mass spectrometry studies, and supplementary figures. This material is available free of charge via the Internet at http://pubs.acs.org.

AUTHOR INFORMATION

Corresponding Author

*E-mail: xwu@cbrc2.mgh.harvard.edu.

Notes

The authors declare no competing financial interest.

ACKNOWLEDGMENTS

This work is supported by Stewart Rahr–MRA (Melanoma Research Alliance) Young Investigator Award, Department of Defense (DoD) Career Development Award (W81XWH-13-1-0203) and MGH Institutional fund (to X. W.). We thank Drs. M. DeRan, Q. Wu, and M. Fukata for reagents and discussions,

DOI: 10.1021/cb500758s
ACS Chem. Biol. 2015, 10, 115–121

and the Taplin Mass Spec Facility at Harvard Medical School for proteomic studies.

REFERENCES

(1) Linder, M. E., and Deschenes, R. J. (2007) Palmitoylation: policing protein stability and traffic. *Nat. Rev. Mol. Cell Biol. 8*, 74−84.
(2) Resh, M. D. (2006) Palmitoylation of ligands, receptors, and intracellular signaling molecules. *Sci. STKE 2006*, re14.
(3) Resh, M. D. (2006) Trafficking and signaling by fatty-acylated and prenylated proteins. *Nat. Chem. Biol. 2*, 584−590.
(4) Roth, A. F., Wan, J., Bailey, A. O., Sun, B., Kuchar, J. A., Green, W. N., Phinney, B. S., Yates, J. R., 3rd, and Davis, N. G. (2006) Global analysis of protein palmitoylation in yeast. *Cell 125*, 1003−1013.
(5) Wan, J., Roth, A. F., Bailey, A. O., and Davis, N. G. (2007) Palmitoylated proteins: purification and identification. *Nat. Protoc. 2*, 1573−1584.
(6) Martin, B. R., and Cravatt, B. F. (2009) Large-scale profiling of protein palmitoylation in mammalian cells. *Nat. Methods 6*, 135−138.
(7) Hang, H. C., Geutjes, E. J., Grotenbreg, G., Pollington, A. M., Bijlmakers, M. J., and Ploegh, H. L. (2007) Chemical probes for the rapid detection of Fatty-acylated proteins in Mammalian cells. *J. Am. Chem. Soc. 129*, 2744−2745.
(8) Smotrys, J. E., and Linder, M. E. (2004) Palmitoylation of intracellular signaling proteins: regulation and function. *Annu. Rev. Biochem. 73*, 559−587.
(9) Rocks, O., Peyker, A., Kahms, M., Verveer, P. J., Koerner, C., Lumbierres, M., Kuhlmann, J., Waldmann, H., Wittinghofer, A., and Bastiaens, P. I. (2005) An acylation cycle regulates localization and activity of palmitoylated Ras isoforms. *Science 307*, 1746−1752.
(10) Cuiffo, B., and Ren, R. (2010) Palmitoylation of oncogenic NRAS is essential for leukemogenesis. *Blood 115*, 3598−3605.
(11) Kummel, D., Heinemann, U., and Veit, M. (2006) Unique self-palmitoylation activity of the transport protein particle component Bet3: a mechanism required for protein stability. *Proc. Natl. Acad. Sci. U.S.A. 103*, 12701−12706.
(12) Duncan, J. A., and Gilman, A. G. (1996) Autoacylation of G protein alpha subunits. *J. Biol. Chem. 271*, 23594−23600.
(13) Lobo, S., Greentree, W. K., Linder, M. E., and Deschenes, R. J. (2002) Identification of a Ras palmitoyltransferase in *Saccharomyces cerevisiae*. *J. Biol. Chem. 277*, 41268−41273.
(14) Roth, A. F., Feng, Y., Chen, L., and Davis, N. G. (2002) The yeast DHHC cysteine-rich domain protein Akr1p is a palmitoyl transferase. *J. Cell Biol. 159*, 23−28.
(15) Greaves, J., and Chamberlain, L. H. (2011) DHHC palmitoyl transferases: substrate interactions and (patho)physiology. *Trends Biochem. Sci. 36*, 245−253.
(16) Saleem, A. N., Chen, Y. H., Baek, H. J., Hsiao, Y. W., Huang, H. W., Kao, H. J., Liu, K. M., Shen, L. F., Song, I. W., Tu, C. P., Wu, J. Y., Kikuchi, T., Justice, M. J., Yen, J. J., and Chen, Y. T. (2010) Mice with alopecia, osteoporosis, and systemic amyloidosis due to mutation in Zdhhc13, a gene coding for palmitoyl acyltransferase. *PLoS Genet. 6*, e1000985.
(17) Yanai, A., Huang, K., Kang, R., Singaraja, R. R., Arstikaitis, P., Gan, L., Orban, P. C., Mullard, A., Cowan, C. M., Raymond, L. A., Drisdel, R. C., Green, W. N., Ravikumar, B., Rubinsztein, D. C., El-Husseini, A., and Hayden, M. R. (2006) Palmitoylation of huntingtin by HIP14 is essential for its trafficking and function. *Nat. Neurosci. 9*, 824−831.
(18) Mill, P., Lee, A. W., Fukata, Y., Tsutsumi, R., Fukata, M., Keighren, M., Porter, R. M., McKie, L., Smyth, I., and Jackson, I. J. (2009) Palmitoylation regulates epidermal homeostasis and hair follicle differentiation. *PLoS Genet. 5*, e1000748.
(19) Mansilla, F., Birkenkamp-Demtroder, K., Kruhoffer, M., Sorensen, F. B., Andersen, C. L., Laiho, P., Aaltonen, L. A., Verspaget, H. W., and Orntoft, T. F. (2007) Differential expression of DHHC9 in microsatellite stable and instable human colorectal cancer subgroups. *Br. J. Cancer 96*, 1896−1903.
(20) Yamamoto, Y., Chochi, Y., Matsuyama, H., Eguchi, S., Kawauchi, S., Furuya, T., Oga, A., Kang, J. J., Naito, K., and Sasaki, K. (2007) Gain of 5p15.33 is associated with progression of bladder cancer. *Oncology 72*, 132−138.
(21) Yu, L., Reader, J. C., Chen, C., Zhao, X. F., Ha, J. S., Lee, C., York, T., Gojo, I., Baer, M. R., and Ning, Y. (2011) Activation of a novel palmitoyltransferase ZDHHC14 in acute biphenotypic leukemia and subsets of acute myeloid leukemia. *Leukemia 25*, 367−371.
(22) Kadowaki, T., Wilder, E., Klingensmith, J., Zachary, K., and Perrimon, N. (1996) The segment polarity gene porcupine encodes a putative multitransmembrane protein involved in Wingless processing. *Genes Dev. 10*, 3116−3128.
(23) Gao, X., Arenas-Ramirez, N., Scales, S. J., and Hannoush, R. N. (2011) Membrane targeting of palmitoylated Wnt and Hedgehog revealed by chemical probes. *FEBS Lett. 585*, 2501−2506.
(24) Zou, C., Ellis, B. M., Smith, R. M., Chen, B. B., Zhao, Y., and Mallampalli, R. K. (2011) Acyl-CoA:lysophosphatidylcholine acyltransferase I (Lpcat1) catalyzes histone protein O-palmitoylation to regulate mRNA synthesis. *J. Biol. Chem. 286*, 28019−28025.
(25) Hannoush, R. N., and Sun, J. (2010) The chemical toolbox for monitoring protein fatty acylation and prenylation. *Nat. Chem. Biol. 6*, 498−506.
(26) Zheng, B., DeRan, M., Li, X., Liao, X., Fukata, M., and Wu, X. (2013) 2-Bromopalmitate analogues as activity-based probes to explore palmitoyl acyltransferases. *J. Am. Chem. Soc. 135*, 7082−7085.
(27) De Vos, M. L., Lawrence, D. S., and Smith, C. D. (2001) Cellular pharmacology of cerulenin analogs that inhibit protein palmitoylation. *Biochem. Pharmacol. 62*, 985−995.
(28) Jochen, A. L., Hays, J., and Mick, G. (1995) Inhibitory effects of cerulenin on protein palmitoylation and insulin internalization in rat adipocytes. *Biochim. Biophys. Acta 1259*, 65−72.
(29) Lawrence, D. S., Zilfou, J. T., and Smith, C. D. (1999) Structure-activity studies of cerulenin analogues as protein palmitoylation inhibitors. *J. Med. Chem. 42*, 4932−4941.
(30) Mani, N. S., and Townsend, C. A. (1997) A concise synthesis of (+)-cerulenin from a chiral oxiranyllithium. *J. Org. Chem. 62*, 636−640.
(31) Jennings, B. C., and Linder, M. E. (2012) DHHC protein S-acyltransferases use similar ping-pong kinetic mechanisms but display different acyl-CoA specificities. *J. Biol. Chem. 287*, 7236−7245.
(32) Noritake, J., Fukata, Y., Iwanaga, T., Hosomi, N., Tsutsumi, R., Matsuda, N., Tani, H., Iwanari, H., Mochizuki, Y., Kodama, T., Matsuura, Y., Bredt, D. S., Hamakubo, T., and Fukata, M. (2009) Mobile DHHC palmitoylating enzyme mediates activity-sensitive synaptic targeting of PSD-95. *J. Cell Biol. 186*, 147−160.
(33) Davda, D., El Azzouny, M. A., Tom, C. T., Hernandez, J. L., Majmudar, J. D., Kennedy, R. T., and Martin, B. R. (2013) Profiling targets of the irreversible palmitoylation inhibitor 2-bromopalmitate. *ACS Chem. Biol. 8*, 1912−1917.
(34) Vartak, N., Papke, B., Grecco, H. E., Rossmannek, L., Waldmann, H., Hedberg, C., and Bastiaens, P. I. (2014) The autodepalmitoylating activity of APT maintains the spatial organization of palmitoylated membrane proteins. *Biophys. J. 106*, 93−105.
(35) Bateman, L. A., Zaro, B. W., Miller, S. M., and Pratt, M. R. (2013) An alkyne-aspirin chemical reporter for the detection of aspirin-dependent protein modification in living cells. *J. Am. Chem. Soc. 135*, 14568−14573.
(36) Pitscheider, M., Mäusbacher, N., and Sieber, S. A. (2012) Antibiotic activity and target discovery of three-membered natural product-derived heterocycles in pathogenic bacteria. *Chem. Sci. 3*, 2035−2042.

DOI: 10.1021/cb500758s
ACS Chem. Biol. 2015, 10, 115−121

ARTICLE
PUBLISHED ONLINE: 22 FEBRUARY 2016 | DOI: 10.1038/NCHEMBIO.2036

Autopalmitoylation of TEAD proteins regulates transcriptional output of the Hippo pathway

PuiYee Chan[1,7], Xiao Han[2–4,7], Baohui Zheng[1], Michael DeRan[1], Jianzhong Yu[5,6], Gopala K Jarugumilli[1], Hua Deng[5,6], Duojia Pan[5,6], Xuelian Luo[3,4]* & Xu Wu[1]*

TEA domain (TEAD) transcription factors bind to the coactivators YAP and TAZ and regulate the transcriptional output of the Hippo pathway, playing critical roles in organ size control and tumorigenesis. Protein S-palmitoylation attaches a fatty acid, palmitate, to cysteine residues and regulates protein trafficking, membrane localization and signaling activities. Using activity-based chemical probes, we discovered that human TEADs possess intrinsic palmitoylating enzyme–like activities and undergo autopalmitoylation at evolutionarily conserved cysteine residues under physiological conditions. We determined the crystal structures of lipid-bound TEADs and found that the lipid chain of palmitate inserts into a conserved deep hydrophobic pocket. Strikingly, palmitoylation did not alter TEAD's localization, but it was required for TEAD's binding to YAP and TAZ and was dispensable for its binding to the Vgll4 tumor suppressor. Moreover, palmitoylation-deficient TEAD mutants impaired TAZ-mediated muscle differentiation *in vitro* and tissue overgrowth mediated by the *Drosophila* YAP homolog Yorkie *in vivo*. Our study directly links autopalmitoylation to the transcriptional regulation of the Hippo pathway.

Hippo signaling plays key roles in organ size control and tumor suppression[1,2]. The signal transduction involves a core kinase cascade, including the MST1/MST2 and Lats1/Lats2 kinases, leading to phosphorylation, cytoplasmic retention and inhibition of YAP and TAZ (hereafter YAP/TAZ)[3]. Physiological or pathological inactivation of these kinases leads to YAP/TAZ dephosphorylation and nuclear accumulation. Subsequently, nuclear YAP/TAZ binds to TEA/TEF (transcriptional enhancer factor)-domain transcription factors (TEAD1–TEAD4 in mammals and Scalloped in *Drosophila*) to mediate target gene expression[3,4]. The TEAD–YAP complex regulates normal development of skin, muscle, lung and liver and is also an oncogenic factor that is amplified in many human cancers[5,6]. TEADs can also bind to Vgll4, which has been implicated as a tumor suppressor through its ability to compete with YAP/TAZ for TEAD binding[7,8]. Therefore, TEADs are essential in regulating the transcriptional output of the Hippo pathway. Although targeting TEAD–YAP could be a promising therapeutic approach for diseases involving deregulation of the Hippo pathway[9], it remains challenging to directly inhibit transcription factors with small molecules. Therefore, understanding the regulation of TEADs might reveal new therapeutic opportunities for drug discovery.

Post-translational S-palmitoylation attaches a 16-carbon fatty acid, palmitate, to the cysteine residue through a reversible thioester bond. Numerous palmitoylated proteins have been identified through proteomic studies[10–14]. Dynamic S-palmitoylation is critical in regulating the trafficking, membrane localization and functions of many proteins, including Src-family kinases, GTPases and synaptic adhesion molecules[15,16]. Asp-His-His-Cys (DHHC) family proteins are evolutionarily conserved protein palmitoyl acyltransferases (PATs)[10] that mediate enzymatic S-palmitoylation[17]. In addition, some proteins can bind to palmitoyl–coenzyme A (palmitoyl-CoA) directly and undergo PAT-independent autopalmitoylation[18]. However, autopalmitoylation is poorly characterized. Most reported examples have been observed under nonphysiological high concentration of palmitoyl-CoA (>100 μM)[19], and to date only a few proteins, including the yeast transporter protein Bet3, have been found to be autopalmitoylated under physiological concentrations of palmitoyl-CoA (1–10 μM)[18,20]. Therefore, it will be important to identify additional autopalmitoylated proteins and to understand their regulation and functions.

Toward this end, we have developed activity-based chemical probes based on irreversible inhibitors of PATs, 2-bromopalmitate (2-BP) and cerulenin, which inhibit palmitoylating activities by alkylating the active site cysteines of the enzymes or autopalmitoylated proteins[21]. We have synthesized analogs of 2-BP and cerulenin with an alkyne tail, which serve as bioorthogonal chemical reporters for covalently labeling and profiling PATs and autopalmitoylated proteins[22,23]. Through proteomic and biochemical studies, we have determined that the TEAD transcription factors are palmitoylated at evolutionarily conserved cysteine residues. We found that TEADs undergo PAT-independent autopalmitoylation at physiological concentrations of palmitoyl-CoA. We determined the crystal structures of the lipid-bound TEADs and revealed a new ligand-binding site in TEADs. Furthermore, we found that autopalmitoylation plays critical roles in regulating TEAD–YAP association and their physiological functions *in vitro* and *in vivo*. Therefore, palmitoylation of TEADs plays important roles in regulating Hippo pathway transcriptional complexes.

RESULTS

TEAD transcription factors are palmitoylated

To detect protein palmitoylation, analogs of palmitate, such as 15-hexadecynoic acid (**Fig. 1a**, **1**), have been widely used as chemical reporters to metabolically label palmitoylated proteins (substrates)[24,25]. To explore PATs and autopalmitoylated proteins, we synthesized the activity-based chemical probes 2-bromohexadec-15-ynoic acid (**2**) and *cis*-2,3-epoxy-4-oxooctadec-17-ynamide

[1]Cutaneous Biology Research Center, Massachusetts General Hospital, Harvard Medical School, Charlestown, Massachusetts, USA. [2]Key Laboratory for Molecular Enzymology & Engineering, Ministry of Education, School of Life Sciences, Jilin University, Changchun, China. [3]Department of Pharmacology, University of Texas Southwestern Medical Center, Dallas, Texas, USA. [4]Department of Biophysics, University of Texas Southwestern Medical Center, Dallas, Texas, USA. [5]Howard Hughes Medical Institute, Johns Hopkins University School of Medicine, Baltimore, Maryland, USA. [6]Department of Molecular Biology & Genetics, Johns Hopkins University School of Medicine, Baltimore, Maryland, USA. [7]These authors contributed equally to this work. *e-mail: xuelian.luo@utsouthwestern.edu or xwu@cbrc2.mgh.harvard.edu

(**3**), respectively[22,23]. We performed labeling, enrichment and proteomic analysis of the probe-labeled proteins and found that **2** and **3** can covalently label >300 proteins, including several known PATs and acyltransferases[22,23].

Among the hits from chemoproteomic studies, we identified the TEAD transcription factors TEAD1 and TEAD3, which had multiple unique matching peptides in proteomic studies (**Supplementary Results**, **Supplementary Fig. 1a**). TEADs bind to the transcription coactivators YAP and TAZ and regulate the transcriptional output of the Hippo pathway[4–6,26], which plays critical roles in organ size control, regeneration and tumorigenesis[1]. To validate that TEADs are palmitoylated, we transfected Myc-TEAD1 and TEAD4 constructs into HEK293A cells, labeled the cells with 50 μM of **1** or **2**, and then performed copper-catalyzed 1,3-dipolar cycloaddition (click reaction) with biotin-azide followed by detection with streptavidin blots. Myc-TEAD1 and TEAD4 were indeed labeled by both probes (**Fig. 1b**), suggesting that TEADs are palmitoylated. To characterize whether endogenous TEAD proteins are palmitoylated, we metabolically labeled HEK293A and MCF10A cells with **1**, performed a click reaction with biotin-azide and then enriched for palmitoylated proteins by streptavidin bead pulldown. We successfully detected all four endogenous human TEADs (TEAD1–TEAD4) in the pulldown samples by western blotting (**Fig. 1c**), indicating that they were indeed palmitoylated in cells. Although TEAD2 and TEAD4 had not been among the hits in chemical proteomics studies, possibly due to their low abundance and our stringent criteria for mass spectroscopic analysis, our detailed biochemical experiments confirmed that all four TEADs should be palmitoylated in cells. Similarly, the *Drosophila* Scalloped protein is palmitoylated (**Supplementary Fig. 1b**), suggesting that TEAD palmitoylation is evolutionarily conserved. In addition, TEAD1 can also be labeled by **3** (**Supplementary Fig. 1c**). Furthermore, treatment with hydroxylamine dramatically reduced the palmitoylation levels in TEAD1, suggesting that TEADs are S-palmitoylated through a reversible thioester linkage (**Fig. 1d**). Taken together, our results indicate that TEAD family transcription factors are S-palmitoylated.

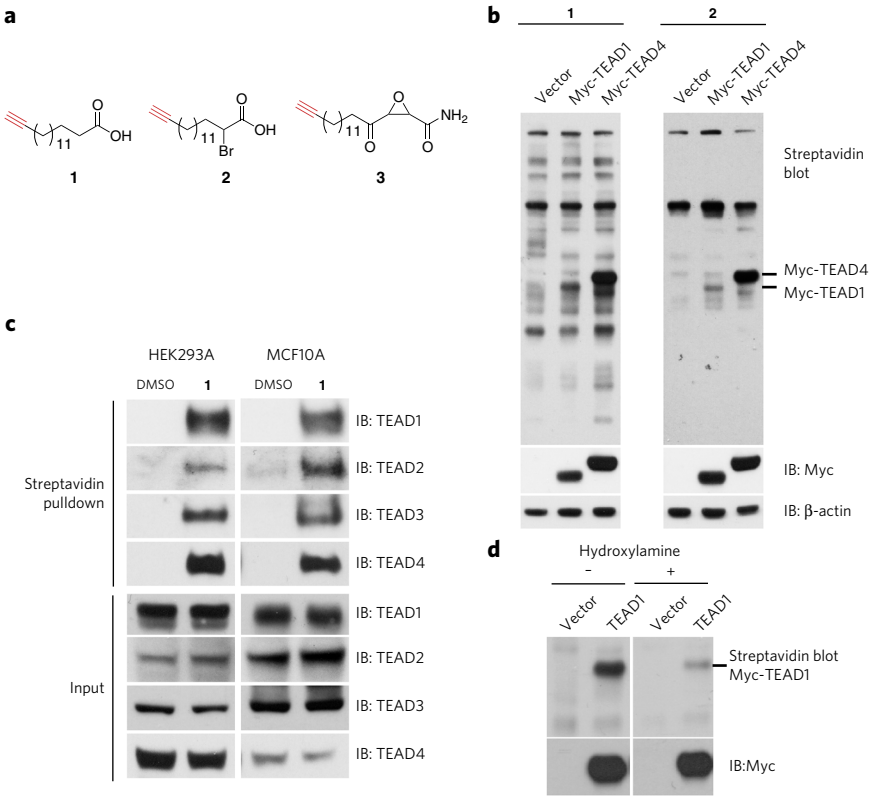

Figure 1 | Chemical approaches reveal that TEA domain (TEAD) transcription factors are palmitoylated. (**a**) Structures of the chemical reporter of palmitoylation, **1**, and the activity-based chemical probes for palmitoyl acyltransferases (PATs) and autopalmitoylated proteins, **2** and **3**. (**b**) Streptavidin blot showing palmitoylation of **1**- and **2**-labeled Myc-TEAD1 and Myc-TEAD4 in HEK293A cells. (**c**) Endogenous human TEAD1–TEAD4 are all palmitoylated. The palmitoylated proteomes of HEK293A and MCF10A cells were labeled with **1**, enriched with streptavidin beads and subjected to western blotting using antibodies to TEAD1–TEAD4. (**d**) TEAD1 is S-palmitoylated, and hydroxylamine treatment dramatically decreased its palmitoylation levels. See **Supplementary Figure 10** for full images of the blots in **c** and **d**.

TEADs are palmitoylated at conserved cysteine residues

To identify the sites of palmitoylation in TEAD, we aligned sequences from the TEAD family of proteins across different species, including human, *Xenopus laevis*, zebrafish, *Drosophila melanogaster* and *Caenorhabditis elegans*. We found that three cysteine residues are evolutionarily conserved (**Supplementary Fig. 2a**) and speculated that these residues might play roles in TEAD palmitoylation. We mutated the three residues to serine in human TEAD1 (producing the C53S, C327S and C359S mutants) and tested whether the mutations affected TEAD1 palmitoylation. All three mutants, and especially C359S, showed decreased palmitoylation (**Fig. 2a**). These results suggest that C359 is critical in TEAD1 palmitoylation and might be a major site of modification. Furthermore, mutation of all three cysteine residues in combination, C53S/C327/C359S (3CS), completely ablated TEAD1 palmitoylation (**Fig. 2b**), confirming that these residues are involved in this process.

TEADs undergo PATs-independent autopalmitoylation

Because TEADs could be labeled by probes **2** and **3** (**Fig. 1b**, **Supplementary Fig. 1c**), we hypothesized that TEADs might possess palmitoylating enzyme–like activities and undergo autopalmitoylation. We had previously purified recombinant TEAD2 protein[27], allowing us to readily carry out *in vitro* experiments using TEAD2. We incubated recombinant human TEAD2 (full-length protein or the YAP-binding domain (YBD), TEAD2 residues 217–447) with a clickable analog of palmitoyl-CoA (15-hexadecynoic CoA) at neutral pH *in vitro* and then carried out a click reaction with biotin-azide followed by streptavidin blotting. Both full-length TEAD2 and the YBD were palmitoylated *in vitro* in the absence of PATs (**Fig. 2c**, **Supplementary Fig. 2b**). In addition, overexpressing each of the DHHC-family PATs did not significantly alter the palmitoylation levels of TEAD1 in cells (**Supplementary Fig. 2c**), confirming that TEAD palmitoylation is independent of PATs. We then carried out intact MS analysis of the recombinant TEAD2 YBD. We identified the peak corresponding to unmodified TEAD2 (26,497 Da) and also, interestingly, a small side peak (26,736 Da) (**Fig. 2d**) that is consistent with a palmitate modification to the protein. These results suggest that a small fraction of the recombinant TEAD2-YBD is palmitoylated when expressed in bacteria. In addition, after incubating TEAD2 YBD with palmitoyl-CoA *in vitro*, we observed that the abundance of the 26,736-Da palmitoylated TEAD2 peak increased significantly (**Supplementary Fig. 3a**), further confirming that TEAD2 can be autopalmitoylated. Moreover,

autopalmitoylation of TEAD2 YBD was confirmed by an acyl-biotin exchange (ABE) assay, which converts S-palmitoylation to stable biotinylation for detection (**Fig. 2e**). With 1 μM of palmitoyl-CoA at neutral pH, TEAD2 YBD was autopalmitoylated within 2 min, and the palmitoylation levels reached saturation after 10 min (**Supplementary Fig. 3b**). To determine the dose-dependency of palmitoyl-CoA, we incubated recombinant TEAD2 YBD with various concentrations of alkyne palmitoyl-CoA for 3 min and determined the reaction rate by quantifying the intensities of streptavidin blots (**Supplementary Fig. 3c**). We estimated that the apparent K_m of palmitoyl-CoA in TEAD2 autopalmitoylation is around 0.8 μM (**Fig. 2f**), which is comparable to the K_m of DHHC-family PATs[28]. Physiological palmitoyl-CoA concentrations within cells range from 100 nM to 10 μM[29]. Therefore, our results suggested that TEAD palmitoylation could indeed occur under normal physiological conditions. To the best of our knowledge, TEADs are the first autopalmitoylated transcription factors identified, linking cellular palmitoyl-CoA levels directly to transcription factor regulation.

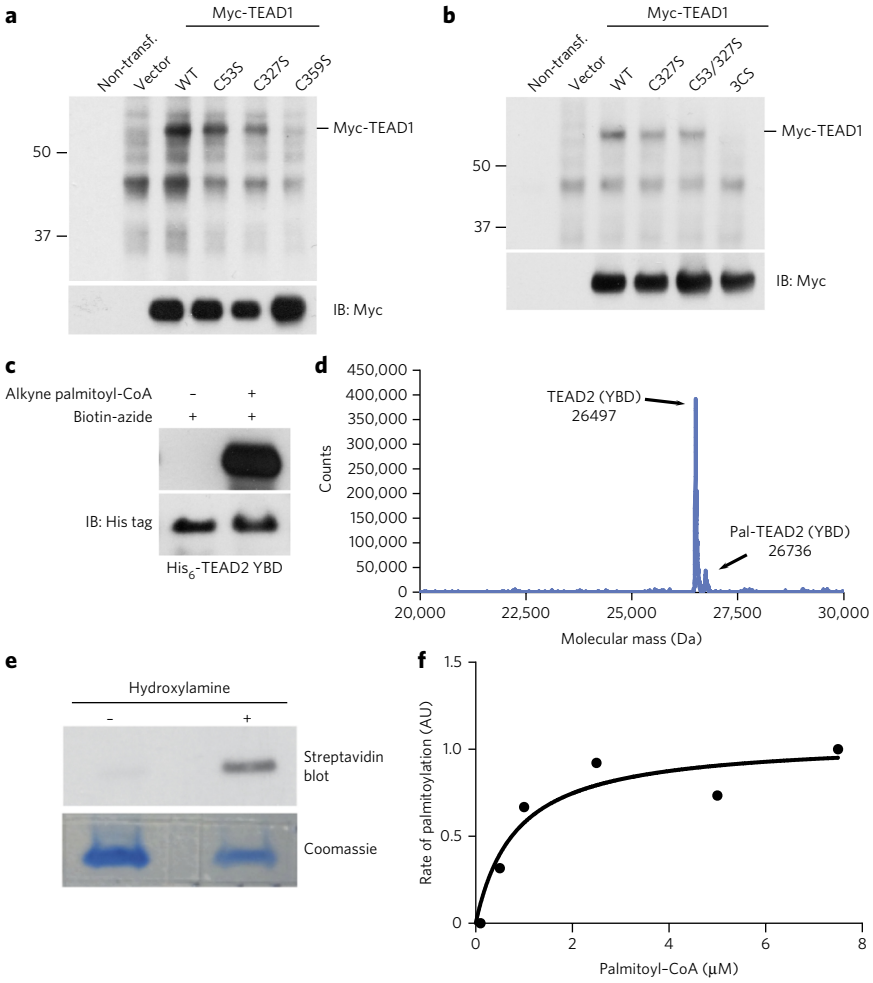

Figure 2 | TEAD is autopalmitoylated at evolutionarily conserved cysteine residues under physiological palmitoyl-CoA concentrations. (**a**,**b**) Mutation of the conserved cysteine residues (C53, C327 and C359) to serine residues individually (**a**) or in combination (**b**) blocked palmitoylation of TEAD1 as seen in streptavidin blots. Molecular weight markers are in kDa. (**c**) Recombinant TEAD2 protein (YAP binding domain, YBD) is autopalmitoylated *in vitro* in the presence of alkyne palmitoyl-CoA. (**d**) Mass spectrometry analysis of recombinant TEAD2 YBD reveals palmitoylation of TEAD2. (**e**) Acyl-biotin exchange (ABE) assay confirmed autopalmitoylation of recombinant TEAD2 YBD. (**f**) The K_m value of palmitoyl-CoA in TEAD2 autopalmitoylation was estimated by plotting the reaction rate against the substrate concentration. See **Supplementary Figure 11** for full images of the blots in **a**–**e**.

Structural analysis of palmitoylation

To reveal the structural basis for the lipid modification of TEADs, we carried out X-ray crystallography studies of TEAD2 YBD ($TEAD2_{217–447}$). We expressed and purified native human TEAD2 YBD from bacteria and determined its structure to a resolution of 2.0 Å (PDB code 5HGU) by molecular replacement with the selenomethionine-labeled TEAD2 YBD (PDB code 3L15)[27] as the search model (**Supplementary Table 1**). We observed clear extra electron density in a deep hydrophobic pocket adjacent to C380 (corresponding to C359 of TEAD1), indicating that TEAD2 binds to an unknown small-molecule ligand. Consistent with our results concerning TEAD2 palmitoylation obtained by the chemical biology methods and MS (**Fig. 2d**), we found that the extra electron density indeed corresponds to a 16-carbon fatty acid (palmitate) (**Fig. 3a**). The lipid chain of palmitate inserts deeply into the pocket, with the free carboxyl group pointing to, but not covalently attached to, C380 of TEAD2. We reasoned that the palmitate might initially be covalently attached to C380, but the labile thioester bond might then be cleaved during purification and crystallization under slightly basic conditions. Consistently, surface drawings of TEAD2 reveal that the carboxyl group of palmitate is solvent accessible through an opening adjacent to C380 (**Fig. 3b**). This opening is also large enough to allow free palmitate to diffuse in and out of the pocket. Interestingly, a recent report on the structure of TEAD2 obtained using slightly different purification conditions resulted in a higher yield of palmitoylated TEAD2, and the covalent bond can be observed in the crystal structures[30].

To explore whether covalent palmitoylation could be observed in other TEAD structures, we revisited the previously reported crystal structures of human TEAD1–YAP complex (PDB code 3KYS), mouse TEAD4–YAP (PDB code 3JUA) and human TEAD1–cyclic YAP (PDB code 4RE1)[31–33]. We have observed that similar lipid-like electron densities are present in all of the conserved deep pocket of these structures. In mTEAD4–YAP, the electron density appeared to be covalently connected to C360 of TEAD4. However, the electron densities in TEAD4–YAP and TEAD1–cyclic YAP are truncated, making it difficult to assign any to palmitate without prior knowledge of palmitoylation (**Supplementary Fig. 4a**,**b**). The TEAD1–YAP complex, which was coexpressed in bacteria and purified as a complex, showed the highest quality of electron density in the hydrophobic pocket. We refined the structure and found that the electron density indeed corresponds to a palmitate, covalently linked to C359 of TEAD1 (**Fig. 3c**). These results are consistent with our biochemical findings that TEAD1 C359 is palmitoylated. Interestingly, the surface opening observed in the TEAD2-alone structure is blocked by the β1 segment of the YAP peptide in the TEAD1–YAP complex (**Fig. 3d**). Therefore, the thioester bond is solvent inaccessible in the complex, a feature that, together with the mild purification and crystallization conditions, might help to preserve the covalent linkage. As there are no PATs present in bacteria, these findings also confirmed our results indicating that TEAD1 is autopalmitoylated. Taking these data together, we have shown that

TEADs have a conserved hydrophobic pocket occupied by a palmitate, revealing a new structural feature of these transcription factors. The lipid-binding pocket is highly conserved among other TEADs[32]. Therefore, palmitate binding could be an important regulatory mechanism for all TEADs.

The structural studies suggested that palmitoylation of TEAD1 C359 (corresponding to TEAD2 C380) is stable and can be crystallized. However, we cannot rule out the possibility that C327 (corresponding to TEAD2 C348) is partially or transiently palmitoylated in cells as shown in our in cell labeling experiments. We purified recombinant the TEAD2 C380S and C348/380S (2CS) mutants. Consistent with the mutagenesis studies in **Figure 2a**,**b**, TEAD2 C380S could still be autopalmitoylated *in vitro*, but TEAD2 2CS could not (**Supplementary Fig. 5**). These results suggest that both C348 and C380 are involved in palmitoylation, and C380 palmitoylation is more stable.

It has been noted before that TEADs are structurally related to phosphodiesterase δ (PDEδ, PDB codes 1KSH and 3T5I)[27,31,32,34], with two β-sheets packing against each other to form a β-sandwich motif. Interestingly, PDEδ has a similar hydrophobic pocket inside the β-sandwich motif, which binds to the farnesyl chain of GTPases[35,36] (**Supplementary Fig. 6**). It is possible that such structural motifs represents a common lipid-binding site and that other proteins with similar motif might also bind to lipid ligands. Interestingly, small-molecule inhibitors of PDEδ can indeed bind to this pocket and inhibit the association of PDEδ and farnesylated Ras proteins, leading to inhibition of Ras activities[37]. Therefore, targeting such lipid-binding sites might lead to new small-molecule inhibitors of important biological pathways.

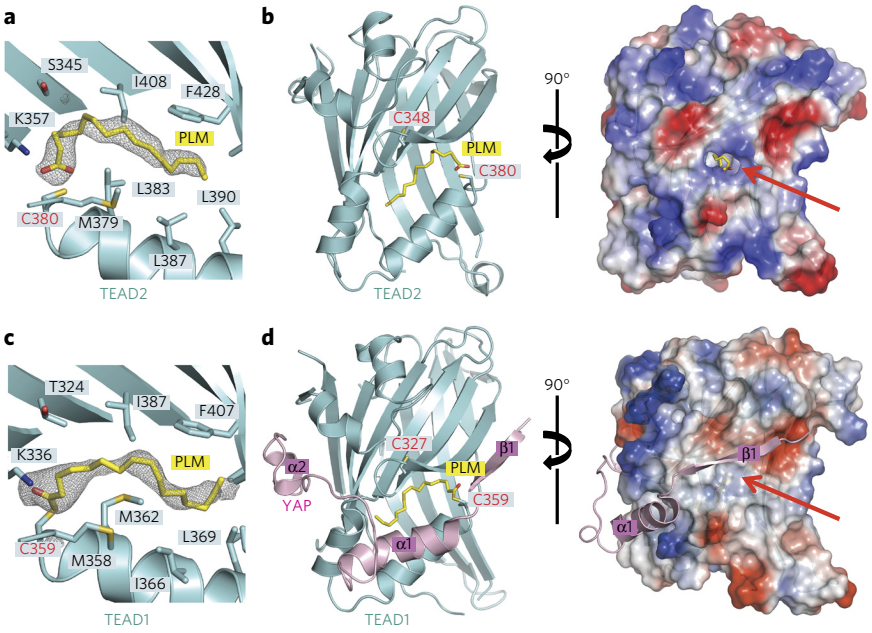

Figure 3 | Structures of palmitate-bound human TEAD2 YBD and TEAD1–YAP complex. (**a**–**d**) The $F_o - F_c$ omit electron density maps for TEAD2 (**a**) and TEAD1–YAP (**c**) at the contour level of 2.5 σ are shown. Palmitate (PLM) is denoted by yellow sticks and surrounding residues by cyan sticks. PLM is covalently linked to C359 of TEAD1 (**c**). Ribbon diagram (left) and electrostatic surface (right) of PLM-bound TEAD2 YBD (PDB code 5HGU) (**b**) and the TEAD1–YAP complex (**d**) are also shown. TEADs are colored in cyan and YAP in pink. Two conserved cysteine residues are indicated. The surface opening in free TEAD2 and the corresponding position in TEAD1–YAP are indicated by red arrows. All structural figures were generated with PyMOL (https://www.pymol.org).

Palmitoylation regulates TEAD-YAP/TAZ association

Although all four TEAD proteins are palmitoylated, we focused on our functional studies on TEAD1 because it is one of the most abundant TEAD proteins ubiquitously expressed. As the palmitoylated cysteine (C359 of TEAD1) is located near the TEAD-YAP interface, we tested whether palmitoylation could allosterically regulate TEAD-YAP association. Indeed, we found that YAP could co-immunoprecipitate with wild-type (WT) TEAD1, but the association was significantly reduced with the palmitoylation-deficient mutants (C359S, 2CS and 3CS) (**Fig. 4a**). In addition, we tested the interaction of TEADs and YAP/TAZ using Gal4-TEAD1 or Gal4-TEAD2 fusion proteins, which can activate a Gal4-responsive luciferase reporter upon YAP or TAZ binding[26,27,31]. We found that WT Gal4-TEAD1 and Gal4-TEAD2 could each activate the Gal4-reponsive luciferase in the presence of YAP or TAZ, indicating the formation of active transcription complexes. However, the palmitoylation-deficient mutants (C359S, 2CS and 3CS) had significantly lower activity (**Fig. 4b**, **Supplementary Fig. 7a**,**b**), with the TEAD 2CS and 3CS mutants in particular showing very little activity. Furthermore, a FRET-based binding assay (Alpha Screen) between TEAD1 and YAP also confirmed that the TEAD mutant (C359S) had weaker association with YAP than WT, and the palmitoylation-deficient mutants (2CS and 3CS) showed almost no binding to YAP (**Fig. 4c**). Taken together, our results indicated that the palmitoylation of TEAD plays important roles in regulating its binding to transcription coactivators. We next examined the functional roles of TEAD palmitoylation. We observed that TEAD1 C359S mutant is partially defective in YAP-induced transcriptional activities. Consistently, TEAD1 2CS or 3CS mutant lost the activities in TEAD-binding element reporter (8xGTIIC-Luc) assays (**Fig. 4d**)[38], suggesting that blocking TEAD palmitoylation impairs its transcriptional activity.

In addition, WT and 3CS mutant TEAD1 localized similarly in the nucleus (**Supplementary Fig. 7c–e**), suggesting that palmitoylation does not alter TEAD1 localization. These findings were consistent with our observations that palmitate binds to a deep pocket inside of TEAD. Unlike other palmitoylated proteins, palmitate might not serve as a membrane anchor for TEADs. Therefore, our results have uncovered new functions of protein palmitoylation in regulating transcription factor complexes.

Moreover, we found that the TEAD2 2CS and 3CS mutants were properly folded. It has been reported that TEADs can bind to Vgll4, a tumor suppressor that competes with YAP for TEAD binding and consequently inhibits YAP oncogenic activity[8]. In the co-immunoprecipitation assay, we found that TEAD1 WT and the palmitoylation-deficient mutants C359S, 2CS and 3CS each bound to Vgll4 (**Fig. 4e**). Consistently, in the FRET-based (Alpha Screen) binding assay, WT and C359S, 2CS and 3CS mutant TEAD1 all bound to Vgll4 similarly (**Fig. 4f**). Taken together, these results showed that palmitoylation is required for TEAD1–YAP binding but is dispensable for TEAD1–Vgll4 binding. In addition, as C359S, 2CS and 3CS TEAD1 mutants are still capable of binding to Vgll4, the loss of YAP binding is not due to misfolding.

In crystal structures, palmitate does not directly interact with YAP. Therefore, palmitate allosterically regulates YAP binding. It has been shown that YAP binds to TEAD through three interfaces[31,32]. Mutations of TEAD residues at interface III greatly inhibit YAP but not Vgll4 binding, suggesting that interface III is more critical for

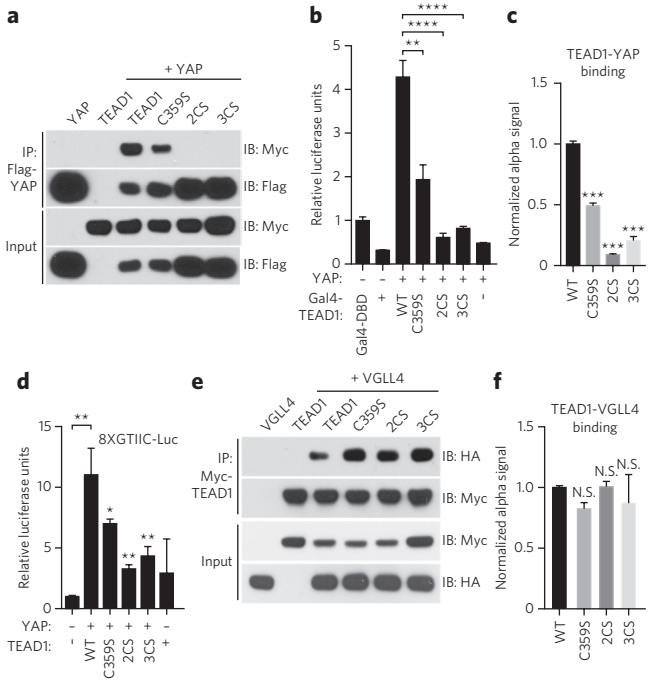

Figure 4 | Palmitoylation of TEAD is required for its association with YAP/TAZ. (**a**) Palmitoylation-deficient mutants of TEAD1 (C359S, 2CS and 3CS) have decreased association with YAP in co-immunoprecipitation (co-IP) experiments. See **Supplementary Figure 12** for full images of the blots. (**b**) YAP binds to and significantly activates WT Gal4-TEAD1 in a Gal4-responsive luciferase assay. The palmitoylation-deficient Gal4-TEAD1 mutants (C359S, 2CS and 3CS) significantly inhibit Gal4-responsive luciferase reporter activities. (**c**) FRET-based binding assay (Alpha Screen) showed that TEAD1 palmitoylation-deficient mutants (C359S, 2CS and 3CS) have decreased binding to YAP, comparing to TEAD1 WT. (**d**) Palmitoylation-deficient mutants of TEAD1 (C359S, 2CS and 3CS) significantly decreased TEAD transcription activity as shown in a TEAD-binding element–driven luciferase reporter assay (8XGTIIC-luciferase). (**e**) Palmitoylation-deficient mutants of TEAD1 (C359S, 2CS and 3CS) retain binding to the Vgll4 tumor suppressor in co-immunoprecipitation (co-IP) experiments. See **Supplementary Figure 12** for full images of the blots. (**f**) FRET-based binding assay (Alpha Screen) showed that TEAD1 palmitoylation-deficient mutants (C359S, 2CS and 3CS) and TEAD1 WT bind to Vgll4 similarly. Data in panels **b**–**d** and **f** are represented as mean ± s.e.m., $n = 3$. P values were determined using two-tailed t-tests. $^{*}P < 0.05$, $^{**}P < 0.005$, $^{***}P < 0.0005$, $^{****}P < 0.0001$; N.S., not significant.

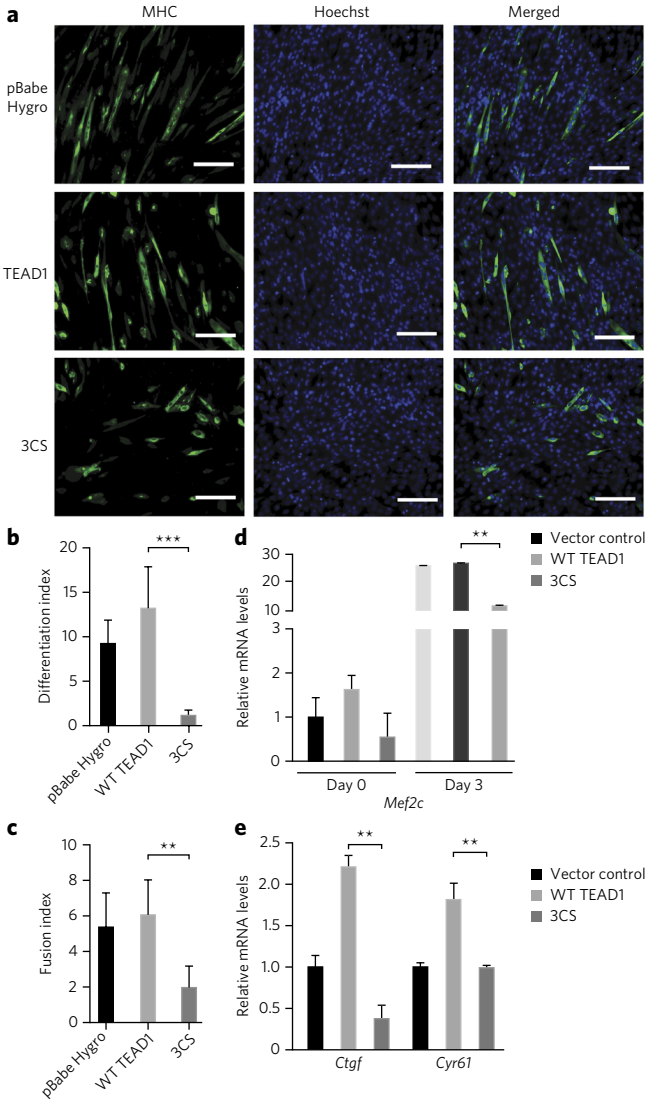

Figure 5 | Palmitoylation regulates TEAD functions in muscle cell differentiation *in vitro*. (**a**) Representative images of myosin heavy chain (MHC, green) immunostaining of C2C12 cells. C2C12 cells stably expressing vector control (pBabe Hygro), TEAD1 WT or the TEAD1 3CS mutant were induced to differentiate for 3 d. Cell nuclei were stained with DAPI (blue). Scale bars, 100 μm. (**b**,**c**) The TEAD1 3CS mutant significantly inhibited myogenic differentiation and myotube fusion. Differentiation and fusion indices were calculated by averaging the data obtained from five different microscope fields from the MHC-stained samples. Data are represented as mean ± s.e.m., $n = 5$. P values were determined using two-tailed t-tests. $^{**}P < 0.005$, $^{***}P < 0.0005$. (**d**,**e**) TEAD 3CS mutant blocked the expression of the myogenic marker *Mef2c* (**d**) before (at day 0) or after (at day 3) the differentiation and TEAD target genes *Ctgf* and *Cyr61* (**e**) in C2C12 cell. RNA samples of C2C12 stably expressing vector control and wild-type and 3CS mutant TEAD1 were collected and cDNA of each was synthesized. mRNA levels of each gene were determined by qRT-PCR using SYBR Green and normalized to *GAPDH*. Data are represented as mean ± s.e.m., $n = 3$. P values were determined using two-tailed t-tests. $^{**}P < 0.01$.

YAP binding[31,32]. We hypothesize that palmitoylation allosterically changes the conformation of TEAD at or near interface III, thus regulating YAP binding but not Vgll4 binding. Our results and a recent report[30] have suggested that binding of palmitate rigidifies the structure of TEAD. We speculate that it might affect the local side chain dynamics around binding interface III, which are required for YAP binding. Further structural and protein side chain dynamic studies using NMR spectrometry will provide more details about how palmitate allosterically regulates TEAD protein dynamics. Interestingly, fatty acylation has been shown previously to allosterically regulate protein functions. For example, N-terminal myristoyl modification of c-Abl binds to the kinase domain and induces conformational changes of the protein, resulted in autoinhibition of c-Abl kinase activity[39,40].

Palmitoylation regulates TEAD physiological functions

We next examined the physiological roles of TEAD palmitoylation. TAZ has been shown to promote terminal differentiation and myotube fusion of skeletal muscle cells through TEAD1 and TEAD4 (refs. 41–43). A TEAD4 mutant (TEAD4-DBD) lacking the YAP/TAZ binding domain functions as a dominant-negative mutant and inhibits C2C12 myoblast differentiation and myotube fusion[41]. Therefore, TEAD–TAZ association is critical for myogenesis. As TEAD palmitoylation is required for TAZ binding, we speculate that loss of TEAD palmitoylation might impair myogenesis.

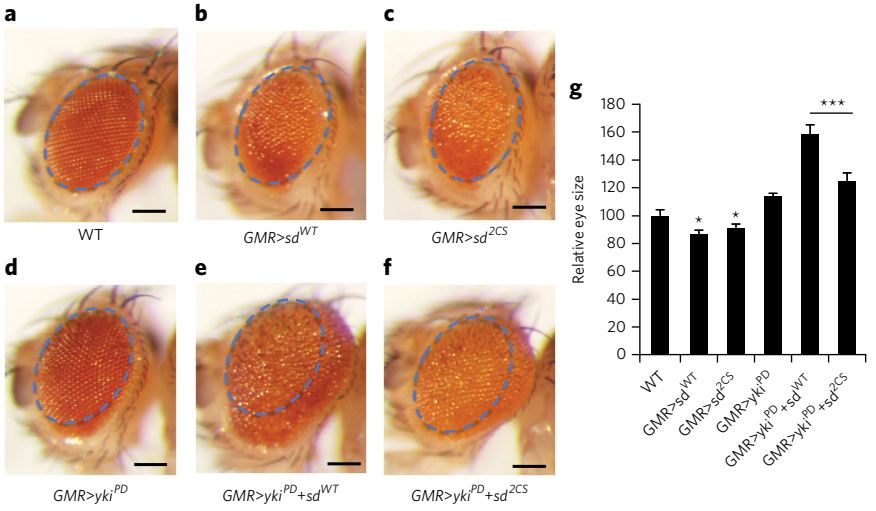

Figure 6 | Palmitoylation is required for the functions of *Drosophila* TEAD protein Scalloped (Sd) *in vivo*. (**a**–**f**) Images of compound eyes from the following genotypes: *GMR-gal4/+* (**a**), *GMR-gal4/UAS-sd^{WT}* (**b**), *GMR-gal4/UAS-sd^{2CS}* (**c**), *GMR-gal4, UAS-yki^{PD}* (**d**), *GMR-gal4, UAS-yki^{PD}/UAS-sd^{WT}* (**e**), *GMR-gal4, UAS-yki^{PD}/UAS-sd^{2CS}* (**f**). Scale bar, 150 μm. Note the overgrowth phenotype (enlarged eyes with rough surface) caused by coexpression of Yki-PD and Sd (WT) (**e**) is compromised when Yki-PD is coexpressed with the palmitoylation-deficient Sd (2CS) mutant (**f**). All images were taken with the same magnification. The size of the eye in WT control flies is marked by the blue dashed line, and the same area is shown in all images to facilitate comparison across genotypes. (**g**) Relative sizes of the fly eyes are quantified in the indicated genotypes. Sd WT and Sd 2CS flies are compared to the wild type, with statistically smaller eyes. Data are represented as mean ± s.e.m., $n = 10$ for each genotype. P values were determined using two-tailed t-tests. $^*P < 0.05$; $^{***}P < 0.001$.

To test this hypothesis, we stably transfected C2C12 myoblast cells with WT or 3CS mutant TEAD1 and then induced them to differentiate. We evaluated muscle differentiation by immunostaining of myosin heavy chain (MHC). The TEAD1 3CS strongly inhibited muscle differentiation and myotube fusion as compared to vector control and WT TEAD1 (**Fig. 5a**, **Supplementary Fig. 8a**). C2C12 cells expressing TEAD1 3CS showed significantly lower differentiation index and fusion index (**Fig. 5b**,**c**). In addition, we observed that expression of the TEAD1 3CS mutant blocked the expression of muscle differentiation genes (*Mef2c*, *MyoG*, *Myh4*), as well as TEAD-specific target genes (*Ctgf* and *Cyr61*), as assessed by qRT-PCR (**Fig. 5d**,**e**, **Supplementary Fig. 8b**,**c**). Taken together, our results suggested that palmitoylation is required for TEADs' normal physiological functions in muscle differentiation *in vitro*.

To further corroborate the functional significance of TEAD palmitoylation, we compared the ability of WT *Drosophila* Scalloped (*Sd*) or a palmitoylation-deficient (2CS) mutant (both constructs targeted to the same genetic locus so as to avoid positional effect of transgene insertion) to cooperate with Yorkie (Yki) in promoting tissue overgrowth using a sensitive *in vivo* assay. Differential splicing of the *Yki* transcript results in two isoforms containing two WW domains (Yki-PG and Yki-PF, Flybase) or a single WW domain (Yki-PD, Flybase). Unlike Yki-PG, whose overexpression resulted in eye overgrowth[5], overexpression of Yki-PD alone resulted in only slightly (but not statistically significantly) larger eye sizes (**Fig. 6a**–**d**). Nevertheless, coexpression of Yki-PD and *Sd* (WT) caused a significant enlargement of eye size (**Fig. 6e**), providing a very sensitive assay for the Scalloped–Yki complex in driving tissue overgrowth. Interestingly, this overgrowth phenotype was significantly compromised when Yki-PD was coexpressed with the palmitoylation-deficient 2CS *Sd* mutant (**Fig. 6f**). We quantified the eye sizes in all the flies and performed statistical analysis of the results (**Fig. 6g**). In addition, the top views of the flies (**Supplementary Fig. 9a**–**f**) showed the size of eyes from a different angle. Interestingly, both *Sd* WT and *Sd* 2CS have statistically significant reduction of eye growth compared to WT flies (**Fig. 6b**,**c**,**g**), which is consistent with the default repressor functions of Scalloped[44]. The difference between *Sd* WT and the 2CS mutant is not statistically significant. Therefore, it is likely that loss of palmitoylation in 2CS *Sd* does not affect its default repressor functions. This result is consistent with our findings in human cells, where 2CS TEAD1 can still bind to Vgll4. To better evaluate the effects on Yki-Sd target genes, we performed qRT-PCR analysis of *Diap1* and *Expanded* in fly S2 cells expressing the 2CS mutant or WT Scalloped. Consistently, expression of Yki and WT Scalloped induced the expression of both genes, while expression of Yki and Scalloped 2CS mutant significantly compromised their expression (**Supplementary Fig. 9g**,**h**). Taken together, our results suggest that palmitoylation is required for the physiological function of the TEAD transcription factors.

DISCUSSION

In summary, using chemical approaches, we have determined that TEADs are specifically autopalmitoylated at evolutionarily conserved cysteine residues. Autopalmitoylation has been considered to be a nonspecific reaction of surface cysteine residues with high concentration of palmitoyl-CoA. However, our studies, together with studies of yeast Bet3 protein, have shown that autopalmitoylation can happen under physiological conditions, with specific cysteine residues being modified. As there are only 23 DHHC-family PATs, it is unlikely that they are responsible for all the palmitoylation activities in cells (more than 1,000 protein substrates are S-palmitoylated). Therefore, it is possible that many S-palmitoylated proteins are modified through PAT-independent processes, and autopalmitoylation could play important roles in regulating protein functions. Our studies have demonstrated, for the first time, the ability to systematically identify autopalmitoylated proteins using chemical tools.

Palmitoylation has commonly been linked to membrane attachment and protein trafficking[10,15]. Our results show that palmitate binds to a hydrophobic pocket in the core of the protein and does not regulate protein membrane binding. It has been noted that in the crystal structures of yeast Bet3, the covalently attached palmitate also binds in a hydrophobic pocket in the protein[45]. Palmitoylation of Bet3 stabilizes the protein and is involved in regulating Bet3 degradation and cofactor binding[18]. Therefore, in addition to providing a membrane-binding moiety, palmitoylation of proteins indeed has other important functions. Further studies of additional autopalmitoylated proteins is likely to reveal new functions of this modification.

We have observed that TEAD1 C359 is the major and stable site of palmitoylation, which is located at the opening of the lipid-binding pocket. We could not purify and crystallize palmitate-free TEAD2, and it is likely that binding of palmitate stabilized the conformation of TEAD, allowing the protein to be crystallized. Nevertheless, TEAD proteins might exist as both palmitoylated and non-palmitoylated species in cells. We have also observed that TEAD2 C380S remains autopalmitoylated, but the C348/380S (2CS) mutant does not, consistent with the observation that TEAD 2CS and 3CS mutants have more significant loss of activity than the C380S mutant. Although we did not observe the lipid

modification of C348 in the crystal structures, which are only snapshots of the most stable conformations of the protein, both C348 and C380 should be involved in palmitoylation. It is possible that C348-palmitoylated TEAD2 has a different conformation, allowing palmitate to bind to the conserved deep pocket. In addition, another hydrophobic pocket near the surface is close to C348 in TEAD2 structure, which could accommodate the binding of hydrophobic ligands, such as bromofenamic acid (BFA)[46]. Further studies would be needed to reveal the detailed structures of C348-palmitoylated TEAD2.

As the levels of TEAD autopalmitoylation are highly relevant to the palmitoyl-CoA concentrations in cells, the cellular palmitoyl-CoA pool might be an upstream regulator of TEAD's activities and the Hippo pathway. Fatty acid synthase (FASN) is the key enzyme that synthesizes palmitoyl-CoA from acetyl-CoA and malonyl-CoA[47]. FASN has been proposed as a potential oncogene, which is upregulated in breast cancers and whose expression is associated with poor prognosis[47]. High level of FASN might lead to high intracellular palmitoyl-CoA, thus promoting TEAD–YAP-mediated oncogenic processes. Further studies would be needed to test whether TEAD–YAP activities are responsible for tumorigenesis in FASN-overexpressed cancer cells. Currently, we do not have evidence showing that TEAD proteins can be palmitoylated and depalmitoylated in a dynamic fashion. Two potential depalmitoylating enzyme families, acylprotein thioesterases (APT1 and APT2) and protein palmitoylthioesterases (PPT1 and PPT2), have been reported[12,16]. It would be interesting to investigate whether these enzymes contribute to TEAD depalmitoylation.

The development of potent and selective small-molecule inhibitors to disrupt TEAD-YAP interaction remains challenging, as the interaction interface is shallow and spans a large area on the surface. Our results showed that the palmitate-binding pocket of TEADs is deep and hydrophobic, ideal for inhibitor binding. Indeed, a recent study has shown that this pocket is accessible to small molecules, although their potency and selectivity are not optimal[46]. Taken together, these results suggest that targeting autopalmitoylation of TEADs by small molecules could be a new strategy for drug discovery.

Received 17 November 2015; accepted 27 January 2016; published online 22 February 2016

METHODS

Methods and any associated references are available in the online version of the paper.

Accession codes. Protein Data Bank (PDB): coordinates for the TEAD2–palmitate complex have been deposited with accession code 5HGU.

References

1. Harvey, K.F., Zhang, X. & Thomas, D.M. The Hippo pathway and human cancer. *Nat. Rev. Cancer* **13**, 246–257 (2013).
2. Pan, D. Hippo signaling in organ size control. *Genes Dev.* **21**, 886–897 (2007).
3. Pan, D. The hippo signaling pathway in development and cancer. *Dev. Cell* **19**, 491–505 (2010).
4. Ota, M. & Sasaki, H. Mammalian Tead proteins regulate cell proliferation and contact inhibition as transcriptional mediators of Hippo signaling. *Development* **135**, 4059–4069 (2008).
5. Wu, S., Liu, Y., Zheng, Y., Dong, J. & Pan, D. The TEAD/TEF family protein Scalloped mediates transcriptional output of the Hippo growth-regulatory pathway. *Dev. Cell* **14**, 388–398 (2008).
6. Zhao, B. *et al.* TEAD mediates YAP-dependent gene induction and growth control. *Genes Dev.* **22**, 1962–1971 (2008).
7. Zhang, W. *et al.* VGLL4 functions as a new tumor suppressor in lung cancer by negatively regulating the YAP-TEAD transcriptional complex. *Cell Res.* **24**, 331–343 (2014).
8. Jiao, S. *et al.* A peptide mimicking VGLL4 function acts as a YAP antagonist therapy against gastric cancer. *Cancer Cell* **25**, 166–180 (2014).
9. Johnson, R. & Halder, G. The two faces of Hippo: targeting the Hippo pathway for regenerative medicine and cancer treatment. *Nat. Rev. Drug Discov.* **13**, 63–79 (2014).
10. Smotrys, J.E. & Linder, M.E. Palmitoylation of intracellular signaling proteins: regulation and function. *Annu. Rev. Biochem.* **73**, 559–587 (2004).
11. Roth, A.F. *et al.* Global analysis of protein palmitoylation in yeast. *Cell* **125**, 1003–1013 (2006).
12. Wan, J., Roth, A.F., Bailey, A.O. & Davis, N.G. Palmitoylated proteins: purification and identification. *Nat. Protoc.* **2**, 1573–1584 (2007).
13. Martin, B.R. & Cravatt, B.F. Large-scale profiling of protein palmitoylation in mammalian cells. *Nat. Methods* **6**, 135–138 (2009).
14. Yount, J.S. *et al.* Palmitoylome profiling reveals S-palmitoylation-dependent antiviral activity of IFITM3. *Nat. Chem. Biol.* **6**, 610–614 (2010).
15. Resh, M.D. Trafficking and signaling by fatty-acylated and prenylated proteins. *Nat. Chem. Biol.* **2**, 584–590 (2006).
16. Fukata, Y. & Fukata, M. Protein palmitoylation in neuronal development and synaptic plasticity. *Nat. Rev. Neurosci.* **11**, 161–175 (2010).
17. Greaves, J. & Chamberlain, L.H. DHHC palmitoyl transferases: substrate interactions and (patho)physiology. *Trends Biochem. Sci.* **36**, 245–253 (2011).
18. Kümmel, D., Heinemann, U. & Veit, M. Unique self-palmitoylation activity of the transport protein particle component Bet3: a mechanism required for protein stability. *Proc. Natl. Acad. Sci. USA* **103**, 12701–12706 (2006).
19. Duncan, J.A. & Gilman, A.G. Autoacylation of G protein alpha subunits. *J. Biol. Chem.* **271**, 23594–23600 (1996).
20. Yang, J. *et al.* Submicromolar concentrations of palmitoyl-CoA specifically thioesterify cysteine 244 in glyceraldehyde-3-phosphate dehydrogenase inhibiting enzyme activity: a novel mechanism potentially underlying fatty acid induced insulin resistance. *Biochemistry* **44**, 11903–11912 (2005).
21. Resh, M.D. Use of analogs and inhibitors to study the functional significance of protein palmitoylation. *Methods* **40**, 191–197 (2006).
22. Zheng, B. *et al.* 2-Bromopalmitate analogues as activity-based probes to explore palmitoyl acyltransferases. *J. Am. Chem. Soc.* **135**, 7082–7085 (2013).
23. Zheng, B., Zhu, S. & Wu, X. Clickable analogue of cerulenin as chemical probe to explore protein palmitoylation. *ACS Chem. Biol.* **10**, 115–121 (2015).
24. Hannoush, R.N. Profiling cellular myristoylation and palmitoylation using ω-alkynyl fatty acids. *Methods Mol. Biol.* **800**, 85–94 (2012).
25. Hang, H.C. & Linder, M.E. Exploring protein lipidation with chemical biology. *Chem. Rev.* **111**, 6341–6358 (2011).
26. Liu-Chittenden, Y. *et al.* Genetic and pharmacological disruption of the TEAD-YAP complex suppresses the oncogenic activity of YAP. *Genes Dev.* **26**, 1300–1305 (2012).
27. Tian, W., Yu, J., Tomchick, D.R., Pan, D. & Luo, X. Structural and functional analysis of the YAP-binding domain of human TEAD2. *Proc. Natl. Acad. Sci. USA* **107**, 7293–7298 (2010).
28. Jennings, B.C. & Linder, M.E. DHHC protein S-acyltransferases use similar ping-pong kinetic mechanisms but display different acyl-CoA specificities. *J. Biol. Chem.* **287**, 7236–7245 (2012).
29. Faergeman, N.J. & Knudsen, J. Role of long-chain fatty acyl-CoA esters in the regulation of metabolism and in cell signalling. *Biochem. J.* **323**, 1–12 (1997).
30. Noland, C.L. *et al.* Palmitoylation of TEAD transcription factors is required for their stability and function in Hippo pathways. *Structure* **24**, 179–186 (2016).
31. Li, Z. *et al.* Structural insights into the YAP and TEAD complex. *Genes Dev.* **24**, 235–240 (2010).
32. Chen, L. *et al.* Structural basis of YAP recognition by TEAD4 in the hippo pathway. *Genes Dev.* **24**, 290–300 (2010).
33. Zhou, Z. *et al.* Targeting Hippo pathway by specific interruption of YAP-TEAD interaction using cyclic YAP-like peptides. *FASEB J.* **29**, 724–732 (2015).
34. Ismail, S.A. *et al.* Arl2-GTP and Arl3-GTP regulate a GDI-like transport system for farnesylated cargo. *Nat. Chem. Biol.* **7**, 942–949 (2011).
35. Zhang, H. *et al.* Photoreceptor cGMP phosphodiesterase delta subunit (PDEdelta) functions as a prenyl-binding protein. *J. Biol. Chem.* **279**, 407–413 (2004).
36. Chandra, A. *et al.* The GDI-like solubilizing factor PDEδ sustains the spatial organization and signalling of Ras family proteins. *Nat. Cell Biol.* **14**, 148–158 (2012).
37. Zimmermann, G. *et al.* Small molecule inhibition of the KRAS PDEδ interaction impairs oncogenic KRAS signaling. *Nature* **497**, 638–642 (2013).
38. Dupont, S. *et al.* Role of YAP/TAZ in mechanotransduction. *Nature* **474**, 179–183 (2011).
39. Nagar, B. *et al.* Structural basis for the autoinhibition of c-Abl tyrosine kinase. *Cell* **112**, 859–871 (2003).
40. Hantschel, O. *et al.* A myristoyl/phosphotyrosine switch regulates c-Abl. *Cell* **112**, 845–857 (2003).
41. Benhaddou, A. *et al.* Transcription factor TEAD4 regulates expression of myogenin and the unfolded protein response genes during C2C12 cell differentiation. *Cell Death Differ.* **19**, 220–231 (2012).

42. Yang, Z. *et al.* Screening with a novel cell-based assay for TAZ activators identifies a compound that enhances myogenesis in C2C12 cells and facilitates muscle repair in a muscle injury model. *Mol. Cell. Biol.* **34**, 1607–1621 (2014).
43. Park, G.H. *et al.* Novel TAZ modulators enhance myogenic differentiation and muscle regeneration. *Br. J. Pharmacol.* **171**, 4051–4061 (2014).
44. Koontz, L.M. *et al.* The Hippo effector Yorkie controls normal tissue growth by antagonizing scalloped-mediated default repression. *Dev. Cell* **25**, 388–401 (2013).
45. Turnbull, A.P. *et al.* Structure of palmitoylated BET3: insights into TRAPP complex assembly and membrane localization. *EMBO J.* **24**, 875–884 (2005).
46. Pobbati, A.V. *et al.* Targeting the central pocket in human transcription factor TEAD as a potential cancer therapeutic strategy. *Structure* **23**, 2076–2086 (2015).
47. Menendez, J.A. & Lupu, R. Fatty acid synthase and the lipogenic phenotype in cancer pathogenesis. *Nat. Rev. Cancer* **7**, 763–777 (2007).

Acknowledgments

This work was supported by a Stewart Rahr–MRA (Melanoma Research Alliance) Young Investigator Award, a Department of Defense (DoD) Career Development Award (W81XWH-13-1-0203), and grants from the American Cancer Society (124929-RSG-13-291-01-TBE), US National Institutes of Health/National Cancer Institute (R01CA181537) (to X.W.), National Institutes of Health/National Institute of Diabetes and Digestive and Kidney Diseases (R01DK107651-01) (to X.W. and X.L.), National Institutes of Health/National Institute of General Medical Sciences (R01GM107415) (to X.L.) and National Institute of Health/National Eye Institute (R01EY015708) (to D.P.); D.P. is supported by the Howard Hughes Medical Institute. We thank N. Bardeesy, M. Fukata, K.-L. Guan and K. White for constructs and cell lines; J.-R.J. Yeh, H. Yu and N. Gray for discussion and critical comments on the manuscript; and the Taplin Mass Spec Core facility at Harvard Medical School and the Proteomics Core at UTSW for proteomic studies. Use of the Argonne National Laboratory Structural Biology Center beamlines at the Advanced Photon Source was supported by the US Department of Energy (DOE) under contract DE-AC02-06CH11357.

Author contributions

X.W. conceived the concepts, designed the experiments and supervised the studies. P.C. designed and performed the cell biology and biochemistry experiments with the help of M.D. X.H. performed protein purification, crystallization and structure determination and carried out MS analysis of TEAD2 autopalmitoylation. B.Z. and G.K.J. synthesized the probes. B.Z. identified TEAD from mass spec studies and tested the DHHC family of PATs. J.Y., H.D. and D.P. carried out *Drosophila* genetics experiments. X.L. contributed to experimental design and structure refinements of palmitate-bound TEAD2 and TEAD1–YAP complex. P.C., D.P., X.L. and X.W. analyzed the data; P.C., D.P. X.L. and X.W. wrote the manuscript with input from all coauthors.

Competing financial interests

The authors declare no competing financial interests.

Additional information

Any supplementary information, chemical compound information and source data are available in the online version of the paper. Reprints and permissions information is available online at http://www.nature.com/reprints/index.html. Correspondence and requests for materials should be addressed to X.L. or X.W.

ONLINE METHODS

Labeling, click reactions and streptavidin pulldown. HEK293A or MCF10A cells were labeled with DMSO or probe **1**, **2** or **3** overnight. Cells were lysed in lysis buffer (50 mM TEA-HCl, pH 7.4, 150 mM NaCl, 1% Triton X-100, 0.2% SDS, cOmplete EDTA-free protease inhibitors) followed by Click reaction with biotin-azide[22]. Proteins were precipitated with 9 volumes of 100% methanol for 2 h or overnight at −20 °C. Proteins were recovered by centrifugation at 14,000 × *g* for 10 min and the precipitates were suspended in suspension buffer (50 mM Tris-HCl, pH 7.7, 150 mM NaCl, 10 mM EDTA, 1% SDS, 0.5% NP-40). Labeled cellular proteins were enriched using streptavidin agarose (Life Technologies) at room temperature with rotation overnight. Protein-bound streptavidin agarose beads were washed three times with suspension buffer without NP-40 and bound proteins were eluted with elution buffer (30 mM D-biotin, 2% SDS, 6 M urea). Samples were processed with SDS-PAGE sample buffer and proteins were resolved by SDS-PAGE. TEAD1–TEAD4 in these samples were detected using TEAD-specific antibodies and streptavidin HRP. Blots were probes with anti-TEAD1 (8526, 1:1,000, Cell Signaling), anti-TEAD2 (8870, 1:1,000, Cell Signaling), anti-TEAD3 (13224, 1:1,000, Cell Signaling), anti-TEAD4 (ab58310, 1:1,000, Abcam) and Streptavidin HRP (1:5,000, Life Technologies). Full images of blots are shown in the supplementary information (**Supplementary Figs. 10–16**).

Cell culture. HEK293A, Phoenix, MCF10A and C2C12 cell lines (obtained from ATCC, Manassas, VA) were grown at 37 °C with 5% CO_2. HEK293A, Phoenix, and C2C12 cell lines were cultured in Dulbecco's modified Eagles media (DMEM) (Life Technologies) supplemented with 10% FBS (FBS) (Thermo/Hyclone, Waltham, MA) and 50 μg/mL penicillin/streptomycin. MCF10A cells were cultured in DMEM/F12 (Life Technologies) supplemented with 5% horse serum, 20 ng/ml EGF, 0.5 μg/ml hydrocortisone, 100 ng/ml cholera toxin, 10 μg/ml insulin and 50 μg/ml penicillin/streptomycin. None of cell lines used in this paper listed in the database of commonly misidentified cell lines maintained by ICLAC. All cell lines are free of mycoplasma contamination.

Transfection and transduction. Plasmids were transfected with jetPRIME (Polyplus transfection) or XtremeGene HP (Roche) according to the manufacturer's instructions.

For retrovirus production, Phoenix cells were transfected with VSV-G and empty pBabe hygro or pBabe hygro containing TEAD1 wild type or 3CS mutant cDNA. Supernatants were collected by centrifugation and filtered through a 0.45 μm syringe filter (Corning) 48 h post-transfection. Cells were infected with 2 ml viral supernatant in the presence of 10 μg/ml polybrene (Millipore). Cells were incubated for 24–48 h before splitting into selection medium.

Site-directed mutagenesis. Mutagenesis was performed using the QuikChange II Site-Directed Mutagenesis kit (Agilent) following manufacturer's instructions.

Co-immunoprecipitation. HEK-293A cells were transfected with the indicated constructs. After 48 h, cells were lysed with lysis buffer (50 mM Tris-HCl, pH 7.3, 150 mM NaCl, 0.5 mM EDTA, 1% Triton X-100, PhosSTOP phosphatase inhibitor cocktail, cOmplete EDTA-free protease inhibitors cocktail). Flag-YAP or Myc-TEAD1 was immunoprecipitated with anti-FLAG M2 magnetic beads (Sigma-Aldrich) or anti-c-Myc antibody (M4439, Sigma-Aldrich), respectively, overnight with rotation at 4 °C. TEAD1 was captured using Protein A/G magnetic resins (Life Technologies). Protein-bound resins were washed three times with lysis buffer and processed with SDS-PAGE sample buffer. Blots were probed with anti-c-Myc (1:5,000, Sigma-Aldrich), anti-HA (1:10,000, Sigma-Aldrich), anti-FLAG M2 (F1804, 1:5,000, Sigma-Aldrich).

FRET-based Alpha screen binding assay. Myc-TEAD1 and Flag-YAP or Flag-VGLL4 were transfected into HEK293A cells and 24 - 48 h post-transfection, cells were lysed with lysis buffer (20 mM Tris-HCl, pH 7.5, 150 mM NaCl, 1 mM EDTA, 1 mM EGTA, 1% Triton X-100, PhosSTOP phosphatase inhibitor cocktail, cOmplete EDTA-free protease inhibitor). Anti-c-Myc acceptor beads (PerkinElmer) were added to each well and incubated for 2 h before addition of anti-FLAG donor beads (PerkinElmer). Samples were incubated overnight in darkness and Alpha signals were recorded using PerkinElmer EnVision plate reader.

Luciferase assay. Gal-UAS-Luc, YAP, Gal4-TEAD1, Gal4-DBD or Myc-TEAD1 and Renilla luciferase control constructs were transfected into 293T cells and 48 h post-transfection, cells were processed using the Dual-Glo luciferase assay system (Promega) following manufacturer's instructions. Luminescence of Firefly and Renilla luciferase activities were quantified using PerkinElmer EnVision plate reader.

Ni-NTA pulldown and acyl-biotin exchange. Recombinant His_6TEAD2 was incubated with Ni-NTA resin (Life Technologies) in PBS for 1 h at 4 °C. Protein-bound resins were washed and then incubated with 50 μM alkyne palmitoyl-CoA for 2 h at 25 °C. Resins were split into two equivalent reactions, washed with PBS and treated with 50 mM NEM (Thermo Scientific) overnight at 4 °C. Samples were incubated with or without 0.5 M hydroxylamine (Sigma-Aldrich) for 1 h at room temperature and then incubated with 1 μM Biotin-BMCC (Pierce Biotechnology, Inc.) for 1 h at room temperature. Samples were washed and processed with SDS-sample buffer. Proteins were resolved by SDS-PAGE and visualized by immunoblotting with streptavidin HRP, anti-His antibody (1:1,000, SAB1306085, Sigma-Aldrich) or Coomassie blue staining.

C2C12 cell differentiation. C2C12 cells were transduced using retrovirus containing vector control (pBabe hygro), or wild type or 3CS TEAD1. Stable expression was selected initially using 600 μg/ml Hygromycin B (Life Technologies) and then decreased to 300 μg/ml for 2 weeks. To induce differentiation, the culture condition was replaced by differentiation medium (DMEM + 2% horse serum + 50 μg/ml penicillin/streptomycin) with medium change everyday.

Immunofluorescence. Cells were fixed with 4% paraformaldehyde and then permeabilized and blocked with 3% (w/v) BSA/PBS + 0.1% Triton X-100 at room temperature for 30 min. Cells were immunostained with anti-myosin (skeletal, fast) chain (M4276, 1:400, Sigma-Aldrich), anti-Yap (1:1,000, Abgent) or anti-c-myc (1:500, Sigma-Aldrich) antibody overnight at 4 °C. Cells were washed three times with PBS + 0.1% Triton X-100 followed by incubation with Alexa Fluor 488 conjugated anti-mouse secondary antibody (1:500, Life technologies) and Hoechst 33258 (1:2,500, Life Technologies) at room temperature for 2 h. Cells were washed again and images were captured using Nikon Digital Sight microscope.

***Drosophila* genetics.** *UAS-yki*^{PD} construct was generated by cloning the *yki* single WW domain isoform (Yki-PD) cDNA into the pUAST vector. *UAS-sd*^{WT} and *UAS-sd*^{2CS} constructs were generated by cloning wild-type *scalloped* (*sd*) or *sd* palmitoylation-deficient (2CS) mutant cDNA into the pUAST-attB vectors. *UAS-yki*^{PD} transgenic fly was created by conventional transposon-mediated transformation. *UAS-sd*^{WT} and *UAS-sd*^{2CS} transgenic flies were created by phiC31-mediated site-specific transformation, using the attP2 site at 51C. *GMR-Gal4* was used for overexpression analysis. All crosses were done at 25 °C. The quantification of fly eyes were carried out by analyzing the eye area in the images[48], and normalized to the control wild type flies. $n = 10$ for each genotypes. The qRT-PCR analysis of *Diap-1* and *Expanded* was carried out using primer sequences previously reported[48].

Protein purification and crystallization. The cDNA encoding human TEAD2 (residues 217–447, $TEAD2_{217–447}$) was cloned into a pET29 vector (EMD Biosciences) that included a C-terminal His_6-tag. The construct was verified by DNA sequencing. The pET29-$TEAD2_{217–447}$ plasmid was transformed into the *E. coli* strain BL21(DE3)-T1^R cells (Sigma) for protein expression. His_6-tagged $TEAD2_{217–447}$ was purified with Ni^{2+}-NTA agarose resin (Qiagen) and then purified by anion exchange chromatography with a resource-Q column followed by size exclusion chromatography with a Superdex 75 column (GE Healthcare). Purified $TEAD2_{217–447}$ was concentrated to 4 mg/ml in a buffer containing 20 mM Tris (pH 8.0), 100 mM NaCl, 2 mM $MgCl_2$, 1 mM TCEP and 5% glycerol.

Crystals of $TEAD2_{217–447}$ were grown at 20 °C using the hanging-drop vapor-diffusion method with a reservoir solution containing 0.1 M HEPES (pH 7.2) and 2.4 M sodium formate. The crystals were cryo-protected with reservoir solution supplemented with 25% glycerol and then flash-cooled in liquid nitrogen.

***In vitro* palmitoylation.** Recombinant GST-TEAD2 or His_6TEAD2 (500 ng) protein was incubated with the indicated concentrations of alkyne palmitoyl-CoA (Cayman Chemical) for 2 h or the indicated time in 50 mM MES, pH 6.4.

The reaction was quenched with 1% SDS followed by Click reaction as described previously. Samples were analyzed by SDS-PAGE and streptavidin HRP. Band intensities obtained from streptavidin blots were quantified using ImageJ (NIH) and the rate of palmitoylation in arbitrary unit was plotted against the concentration of palmitoyl-CoA. The data was fitted to the Michaelis-Menten equation using Prism v.6.0 (GraphPad). For mass spectrometry analysis, recombinant TEAD2 YBD (1 mg/ml) was incubated with 1 eq. of palmitoyl-CoA for 30 min at room temperature in a buffer containing 50 mM MES, pH 6.4.

Data collection and structure determination. Diffraction data were collected at beamline 19-ID (SBC-CAT) at the Advanced Photon Source (Argonne National Laboratory) at the wavelength of 0.9791 Å at 100 K and processed with HKL3000. Phases were obtained by molecular replacement with Phaser using the crystal structure of human TEAD2 (PDB code 3L15) as the search model. Iterative model building and refinements were carried out with COOT and Phenix, respectively. MolProbity was used for structure validation to show that all models have good geometry. Data collection and structure refinement statistics are summarized in **Supplementary Table 1**. Ramachandran statistics (favored/allowed/outlier (%)) are 97.4/2.6/0.0. The crystal structure of palmitate-bound TEAD1–YAP was obtained by building two thioester-linked palmitate molecules into TEAD1–YAP (PDB code 3KYS) with COOT using the electron density map calculated from 3KYS structure factor. The final model was refined with Phenix.

Statistical analysis. No statistical method was used to predetermine sample size. The experiments were not randomized. For biochemical experiments we performed the experiments at least three independent times. Experiments for which we showed representative images were performed successfully at least 3 independent times. No samples or animal were excluded from the analysis. The investigators were not blinded to allocation during experiments and outcome assessment. All P values were determined using two-tailed t-tests and statistical significance was set at $P = 0.05$. The variance was similar between groups that we compared.

48. Sorrentino, G. *et al.* Metabolic control of YAP and TAZ by the mevalonate pathway. *Nat. Cell Biol.* **16**, 357–366 (2014).

doi:10.1038/nchembio.2036